

**THEORETICAL DETERMINATION OF LITHIUM DIMER  
AND CESIUM DIMER UNDER A MODIFIED MOLECULAR  
ATTRACTIVE POTENTIAL MODEL**

**BY**

**AKANBI, TITILAYO ALICE**

**(19PGCG000078)**

**A Dissertation Submitted to the Department of Physical  
Sciences, College of Pure and Applied Sciences, Landmark  
University, Omu Aran, Kwara State, Nigeria.**

**IN PARTIAL FULFILMENT OF THE  
REQUIREMENTS OF THE AWARD OF MASTER OF  
SCIENCE (M.Sc.) DEGREE IN PHYSICS**

**OCTOBER, 2021.**

## Declaration

I, Titilayo Alice AKANBI, a M.Sc. degree student in the Department of Physical Sciences (Physics Programme), Landmark University, Omu-Aran, hereby declare that this dissertation entitled “THEORETICAL DETERMINATION OF LITHIUM DIMER AND CESIUM DIMER UNDER A MODIFIED MOLECULAR ATTRACTIVE POTENTIAL MODEL”, submitted by me is based on my original work. Any materials obtained from any other persons or institutions have been duly acknowledged.

AKANBI, TITILAYO ALICE.

(19PGCG000078)

.....

Signature & date

## Certification

This is to certify that this dissertation has been read and approved as meeting the requirements of the Department of Physical Sciences, Landmark University, Omu-Aran, Nigeria, for the Award of Master Degree in Physics.

.....  
PROF.J.O. ADENIYI  
(Supervisor) .....  
Date

.....  
DR. C.A ONATE  
(Co-Supervisor) .....  
Date

.....  
DR. A. A. INYINBOR  
(Head of Department) .....  
Date

.....  
.PROF.K.J OYEWUMI  
(External Examiner) .....  
Date

## **Dedication**

This dissertation is dedicated to the Almighty God who daily loads me with His benefits.

## **Acknowledgements**

I want to appreciate God for the gift of life, I adore you Lord. I will never be ungrateful to you Lord. My joy knows no bound in acknowledging the ones that assisted me in one way or the other in the completion of my dissertation.

I want to sincerely appreciate my supervisors, Prof. J.O. Adeniyi and Dr. C. A. Onate who taught me the rudiments of this study and painstakingly went through this write-up to ensure the accuracy of this dissertation. I am grateful sirs. God Almighty will reward your labour of love on me. I thank the Head of Department, Physical Sciences, Dr. A. A. Inyinbor for her encouraging words which has been of help during the seminar presentations. I am grateful to you ma. My heartfelt gratitude goes to the Postgraduate Coordinator, Dr. S. O. Ikubanni for taking time to advise me during seminar presentations which has indeed help me greatly. God will reward you abundantly. I also appreciate all the Faculty and staff of the Department of Physical Sciences: Prof. O.S. Bello, Prof. B.O. Adebessin, Dr. O. Adebimpe, Dr S.J. Adebisi, Dr. S.C Falade, Dr. S. O. Salawu, Dr. E. O. Davids, Mr. L.S. Adebisi, Mr. D.B. Olanrewaju, Mr. K.O..Dopamu, Mrs. E.A. Alejowo, Mr. J. O. Okoro, Mr. M. O. Oluwayemi, Mrs. O. Y. Oludoun, Mrs. B.B. Aladeitan, Mrs. B. Lawal-Adedoyin and others for the assistance they rendered throughout my M.Sc. programme.

Also, to my sister Mrs. O.Y. Oludoun for her accommodation and nurture in all ramifications during my stay, her undaunted support and encouraging words are well appreciated, God will bless and favour you in all your ways. Mrs. O.E. Abiodun, is also appreciated for her kind support during my stay, the Lord will grant your heart desires.

My appreciation also goes to the principal and the entire staff of Federal Government Girls' College Kabba for the permission granted to me to pursue my career, may the Lord promote you all and the College.

To crown it all, my profound gratitude goes to my amiable husband, Engr. O.S Akanbi for conceiving this 'idea' and ensuring it materialises. Your soothing words, provisions, tutelage, love and prayers cannot be forgotten. I am grateful sir, may the Lord Almighty reward all your labour of love and promote you sir. I also appreciate my wonderful children; Philip, Peter and Priscilla for their understanding, moral support and prayers. God will bless you all in Jesus' name. I also appreciate my brother-in-law, Akanbi Muyiwa and Engr. and Mrs. Amole for taking care of my children whenever I am not around, may God grant your request. I also appreciate my dad, erudite O.A. Ogunsanya and my siblings for their encouraging words and prayers throughout this program, may the Lord bless you all.

## Abstract

In the fields of quantum mechanics, the usefulness of molecular potential cannot be over emphasised due to its applications in evaluating diatomic molecules properties and the dynamic behaviour of molecules. Therefore, theoretical investigation was carried out on lithium dimer and cesium dimer under a modified molecular attractive potential model to obtain the solution of the approximate radial Schrödinger equation. Also, the thermodynamic properties of the molecular attractive potential were examined under various conditions.

The goal of this study was to solve the radial Schrödinger equation for molecular attractive potential with the aid of Nikiforov-Uvarov method. The solution was used to acquire the energy equation, energy eigenvalues and its corresponding wave function for the system. Then, the effects of thermodynamic properties such as vibrational partition function, vibrational mean energy, vibrational specific heat capacity, vibrational entropy and vibrational free energy of the molecular attractive potential were examined using specific parameters such as dissociation energy, an equilibrium bond length and special screening parameter. The Rydberg-Klein-Rees were computed and evaluated with experimental values for the cesium dimer molecule and lithium dimer molecule.

From the study, it was observed that as the dissociation energy of the system was increasing, the energy of the system was also increasing. Also, the energy of the system initially increased and later decreased as the quantum numbers were increasing. In addition, the energy of this system were decreasing as the equilibrium bond length was increasing. Furthermore, the impact of the screening parameter was that the energy of the system increased and later decreased to a negative value.

Mathematical procedures were employed to generate the eigenvalues and its corresponding wave functions; the spectroscopic parameters were inputted into the energy equation to obtain

the calculated Rydberg-Klein-Rees values which were compared with the experimental values which, in turn, agreed qualitatively with the theoretical findings.

# Table of Contents

Declaration	ii
Certification	iii
Dedication	iv
Acknowledgements	v
Abstract	vii
Table of Contents	ix
List of Tables	xi
List of Figures	xii
CHAPTER ONE	1
INTRODUCTION	1
1.1 Background of the Study.	1
1.2 Statement of the Problem	2
1.3 Justification for the Study	3
1.4 Aim and Objectives	3
1.5 Research Questions	3
1.6 Scope of the Study	4
1.7 Significance of the Study	4
1.8 Definition of Terms.	4
1.8.1 Dimer.	
1.8.2 Diatomic molecules	5
1.8.3 Cesium	5
1.8.4 Lithium	5
CHAPTER TWO	6
LITERATURE REVIEW	6
2.1 Conceptual Issues.	6
2.2 Review of Some Related Works.	9
2.2.1 Derivation of Schrödinger wave equation	9
2.2.2 The time-independent Schrodinger equation	10
2.3 Gaps identified in the literature.	11
CHAPTER THREE	17
RESEARCH METHODOLOGY	17
3.1 Parametric Nikiforov- Uvarov Method	17
3.2 Solution of radial Schrödinger equation.	21
3.3 The Molecular Attractive Potential and Thermodynamic Properties	25

3.3.1	Vibrational mean energy.	27
3.3.2	Vibrational Specific heat capacity	28
3.3.3	Vibrational entropy	29
3.3.4	Vibrational free energy	29
CHAPTER FOUR		30
RESULTS, DISCUSSION OF RESULTS AND FINDINGS		30
4.1	Results	30
4.2	Discussion of Results	48
4.3	Findings	53
CHAPTER FIVE		55
SUMMARY, CONCLUSION AND RECOMMENDATION		55
5.1	Summary	55
5.2	Conclusion	56
5.3	Recommendation	56
5.4	Contributions to Knowledge	56
REFERENCES		58

## List of Tables

- Table 4.1: Energy spectrum ( $E_{n,\ell}$ ) for various  $n$  and  $\ell$  states with four various values of the dissociation energy with  $\mu = \hbar = 1$ ,  $\alpha = 0.25$ ,  $r_e = 0.20 \text{ \AA}$  and  $\lambda_o = 2$ . 43
- Table 4.2: Energy spectrum ( $E_{n,\ell}$ ) for various states with four different values of the equilibrium bond length  $r_e$  ( $\text{\AA}$ ). 44
- Table 4.3: Energy spectrum ( $E_{n,\ell}$ ) for different  $n$  and  $\ell$  states with four different values of the screening parameter with dissociation energy of 10 and  $\mu = \hbar = 1$ ,  $r_e = 0.20 \text{ \AA}$  and  $\lambda_o = 2$ . 45
- Table 4.4: Comparison of RKR ( $\text{cm}^{-1}$ ) data with calculated energies of  $\text{Cs}_2$  molecule and  $\text{Li}_2$  molecule. 47

## List of Figures

Figure 4.1: Variation of Energy (J) against potential strength A.	30
Figure 4.2: Variation of energy (J) against potential strength B.	31
Figure 4.3: Variation of energy (J) against potential strength C.	32
Figure 4.4: The graph of vibrational partition function versus the maximum quantum state $\lambda$ .	33
Figure 4.5: The graph of vibrational partition function versus the temperature parameter $\beta$ .	34
Figure 4.6: The behaviour of vibrational mean energy U (J) with the maximum quantum state $\lambda$ .	35
Figure 4.7: The plot of vibrational mean energy U (J) against the temperature parameter $\beta$ .	36
Figure 4.8: The behaviour of vibrational specific heat capacity ( $\text{Jkg}^{-1}\text{K}^{-1}$ ) against the maximum quantum state $\lambda$ .	37
Figure 4.9: The behaviour of vibrational specific heat capacity ( $\text{Jkg}^{-1}\text{K}^{-1}$ ) against temperature parameter $\beta$ .	38
Figure 4.10: Variation of vibrational entropy ( $\text{JK}^{-1}$ ) against the maximum quantum state $\lambda$ .	39
Figure 4.11: The plot of vibrational entropy ( $\text{JK}^{-1}$ ) against temperature parameter $\beta$ .	40
Figure 4.12: The plot of vibrational free energy (J) against maximum quantum state $\lambda$ .	41
Figure 4.13: The plot of vibrational free energy (J) against the temperature parameter $\beta$ .	42

# CHAPTER ONE

## INTRODUCTION

### 1.1 Background of the Study.

The description of physics that prevailed before relativity theory is described in classical physics which contains numerous natural features with a regular dimension and quantum theory of low magnitude for natural traits (atomic and sub-atomic). (Jaeger, 2014). As soon as new experimental techniques to the point of investigating atomic and subatomic structures were established, it turned out that classical physics failed miserably to provide the correct explanation for many newly discovered phenomena. It was thus clear that at the microscopic level, the relevance of classical physics ceased and that new ideas had to be invoked to discuss how atoms and molecules are made and how light interacts with them. Classical physics has not been able to clarify many microscopic phases, such as radiation from the black body, photo electrically-powered effects, atomic stability and atomic spectroscopy (Zettili, 2009).

Quantum mechanics is an important physical theory describing nature's physical characteristics at microscopic levels of atoms and subatomic particles (Richard *et al.*, 1964). It is the foundation of quantum field theory, quantum technology, and quantum physics. One of the essential aspects of quantum mechanics is the wave equation that describes some quantum mechanical systems.

The wave equation is a partial differential equation which can confine some scalar functions  $u = u(x_1, x_2, \dots, x_n; t)$  with one or more dependent variables and a time parameter (t)  $x_1, x_2, \dots, x_n$ . For example, the amount of u can be the fluid pressure or the shifting of the vibrating solid particles from their resting locations in a certain specified direction.

The wave equation by itself does not suggest physical solutions; a unique solution usually is found when an extra condition problem like initial conditions is given for the wave amplitude and phase. Another major difficulty is in closed spaces, determined by boundary terms where solutions are like the harmonics of musical instruments, which represent standing waves or harmonics. A hyperbolized differential equation is the simplest example. These changes play key roles in continuum mechanics, quantum mechanics, plasma physics, general relativity, geophysics and many more fields of science and technology.

The wave equation is denoted as:

$$\psi = e^{i(kx-wt)}. \quad (1.1)$$

However, wave equation has two forms which are; relativistic and non-relativistic wave equations. The relativistic wave equation speculates the attitude of particles at high energies and velocities akin to the speed of light. Their energy equation are usually represented in quadratic form. Examples of relativistic wave equation are; Dirac equation and Klein Gordon equation, while the non-relativistic wave equation forecasts the way particles behave when they propagate at a speed less than the speed of light. The example of non-relativistic wave equation is the Schrödinger equation. This research will be limited to the non-relativistic wave equation.

## 1.2 Statement of the Problem

Several researches have been carried out on different kinds of potentials and their applied scientific and engineering uses. However, due to the disparity in the early theoretical results presented and the experimental outcomes, an improved modification in the potentials is essential. Though few potentials have been improved in order to enhance their deficiency with little or no attention paid to the molecular type potential. Therefore, this study focuses on the modified four- parameter exponential type molecular potential which will be used to generate energy equation. The molecules are significant to the chemical physics and molecular physics

in providing an accurate prediction of the potential energy inter atomic function and molecular electronic structure. As such, the cesium dimer and lithium dimer Rydberg-Klein-Rees shall be computed and checked with the results of the experiment due to the presence of spectroscopic parameters in molecular attractive potential.

### **1.3 Justification for the Study**

The importance of molecular potentials in the areas of science and engineering most especially molecular physics, atomic physics, nuclear physics and others cannot be over emphasized. This has contributed greatly to the advancement of quantum physics, chemical physics and other related areas. Therefore, this study was inspired by the scientific applications of molecular potential for the compact molecular description such as calculation of thermodynamic functions, the reaction of gas phase with modelling of the equilibrium constant, etc. As such, this study will investigate the thermodynamic properties of molecular potential and a potential with four parameters of the exponential type that will be used to verify experimental results.

### **1.4 Aim and Objectives**

This study aims to formulate a molecular attractive potential that will be used to study the numerical values of some molecules (cesium dimer and lithium dimer).

The specific objectives are to;

1. obtain the approximate solution of the radial Schrödinger equation of the modified potential;
2. calculate the thermodynamic properties of the molecular attractive potential and
3. verify the theoretical results with experimental results.

### **1.5 Research Questions**

The following questions are expected to be answered by this study:

1. how do we obtain the approximate solutions of the radial Schrödinger equation?
2. how can we compute the properties of thermodynamics of the molecular attractive potential?
3. can the theoretical results juxtapose the experimental results?

## **1.6 Scope of the Study**

The goal of this research is to use a molecular attractive potential to investigate the numerical values of various molecules (cesium dimer and lithium dimer). The study is restricted to the experimental results where secondary data on already established results are used for the numerical computations.

## **1.7 Significance of the Study**

This work is to extend the boundaries of knowledge by the theoretical determination of Rydberg-Klein-Rees (RKR) values of some molecules with a four-parameter-exponential-type molecular potential. Results obtained in this study are good indices that can aid some decisions on methods, parameters and favourable molecular potential which can be used for situating experimental results.

## **1.8 Definition of Terms.**

### **1.8.1 Dimer**

A dimer is an oligomer consisting of two monomers joined by bonds that can either be strong or weak, covalent or intermolecular.

### **1.8.2 Diatomic molecules**

Diatomic molecules are molecules composed of only two atoms, of the same or different chemical elements which can either be homonuclear diatomic molecules or heteronuclear diatomic molecules.

### **1.8.3 Cesium**

Cesium is a chemical element with the symbol Cs and atomic number 55. It is a soft, silvery-golden alkali metal with a melting point of 28.5 °C (83.3 °F), which makes it one of only five elemental metals that are liquid at or near room temperature. Cesium dimer is written as  $Cs_2$

### **1.8.4 Lithium**

Lithium is a chemical element with the symbol Li and atomic number 3. It is a soft, silvery white alkali metal. Under standard conditions, it is the lightest metal and the lightest solid element. Lithium dimer is written as  $Li_2$ .

# CHAPTER TWO

## LITERATURE REVIEW

### 2.1 Conceptual Issues.

Schrödinger wave equation is a partial differential equation that demonstrates how the physical system's quantum status evolves over time. The Schrödinger equation answer goes beyond describing massive systems, as well as molecular and atomic structure systems but potentially even the world in general (Schrödinger, 1926). Schrödinger equation is widely used in sciences such as physics, mathematics and chemistry.

The Schrödinger equation is given as:

$$i\hbar \frac{\partial \psi}{\partial t} = \left[ -\frac{\hbar^2}{2m} \nabla^2 + V(x) \right] \psi(x, t), \quad (2.1)$$

where

$$\nabla^2 = \frac{\partial^2}{\partial x^2} + \frac{\partial^2}{\partial y^2} + \frac{\partial^2}{\partial z^2}, \quad (2.2)$$

$\nabla^2$  is a laplacian operator,

$\psi(x, t)$  is a wave function (amplitude),

$m$  is the mass of the material particle,

$V(x)$  is the potential energy,

$\hbar$  is the reduced Planck's constant,

$\mu$  is the reduced mass of the diatomic molecule.

Rydberg – Klein – Rees is a method used for the production of diatomic molecules empirical potential energy curves for experimental information for vibrational values and rotations.

Hu *et al.*, (2013) indicated that improved exponential-type deformed parameter was developed using energy dissociation and equilibrium bond length as exact diatomic parameters. The screening parameter used in modeling molecular potential functions are unique because it will

be calculated with the aid of parameters like vibrational frequency, Lambert function and some other spectroscopic parameters.

A lot of researches have been carried out on the bound states of the radial Schrödinger equation of various diatomic molecules with different physical potentials. Some of the physical potentials that have received attention are ; Tiez Hua potential (Hamzavi *et al.*, 2012), Kratzer potential (Ikot *et al.*, 2019), Hyperbolic- sinus potential (Onate *et al.*, 2019), Pöschl-Teller type potential (Yahya and Oyewumi, 2016), Hulthén potential (Jia *et al.*, 2008), Hulthén plus generalized exponential coulomb potential (Okon and Popoola, 2015), Generalized hyperbolic potential (Okorie *et al.*, 2019), Inversely Quadratic Yukawa plus Inversely Quadratic Hellman potential (Ita *et al.*, 2013), Improved Rosen Morse potential (Jia *et al.*, 2008 ; Udoh *et al.*, 2019), Manning Rosen potential (Wei and Dong, 2010; Ikhdair, 2011), Generalized Pöschl Teller and hyperbolic potential (Onate and Idiodi, 2016), General molecular potential (Ikot *et al.*, 2018), modified Rosen–Morse potential (Tang *et al.*, 2014), Modified Pöschl potential (Agboola. 2010), Woods- Saxon Potential (Feizi *et al.*, 2011) , Modified Mobius Square Potential (Ikot *et al.*, 2016) , Modified Yukawa potential (Okorie *et al.*, 2018) Screened Kratzer potential (Ikot *et al.*, 2019), q-deformed exponential type potential (Onate *et al.*, 2020), q-deformed Woods–Saxon plus Modified Coulomb potential (Okon and Popoola, 2015), Gaussian Potential (Omugbe *et al.*, 2020), Hartmann potential (Hamzavi *et al.*, 2010). However, there are different methods of solving Schrödinger equation with various physical potential models.

Nikiforov-Uvarov (NU) method, this technique aims at reducing linear differential equation of a second order to a general hypergeometric equation (Nikiforov and Uvarov, 1988; Bera, 2013). The method provides precise solutions with respect to different orthogonal functions, and associated energy eigen values and also its application to relativistic and non-relativistic

(Ikhdair *et al.*, 2009). Recently, this method was simplified by Tezcan and Sever (2008) to parametric Nikiforov-Uvarov.

Asymptotic Iteration Method (AIM) uses an appropriate variables modifications of the Schrödinger equation by reducing it into a hypergeometric differential equation, and it can then be transformed into an equation of second order differential. (Nugraha *et al.*, 2017; Ismail and Saad. 2020). The procedure was more effective when the statistical features of dynamic problem solutions were expanded into a power of a small parameter which is essentially a proportion of the correlation between random impacts.

The functional analysis approach (FAA) or modified factorization method is a second order, homogeneous linear differential equation, which can be utilized to solve a Schrödinger equation and changed into a hypergeometric equation with using the required transformation (Falaye *et al.*, 2014).

Traditional method is used when the exact solution of quantum systems is to be acquired to accomplish this, a second order differential equation is employed to convert the quantum systems to an ordinary differential equation that have unique functions like the confluent hypergeometric functions, associated Laguerre polynomials and others (Dong *et al.*, 2008).

Shape invariance of potentials is used to find eigenvalues and eigenfunctions of different Hamiltonians. These depend crucially assuming a system with a negligible lowest energy which is not possible without supersymmetry and invariant potentials of the form are given where the parameter values spontaneously depart supersymmetry. However, there are two variations of shape invariance, the first step uses two-step shape invariance to estimate the spectrum and eigenstates for systems with broken supersymmetry and it transforms the initial super potential with broken supersymmetry becoming one in which supersymmetry is not broken while the second step uses supersymmetry to determine the spectrum (Asim *et al.*, 2018).

## 2.2 Review of Some Related Works.

### 2.2.1 Derivation of Schrödinger wave equation

The time-dependent Schrödinger wave equation

In a particle with an unlimited potential, it was found that the wave function of a fixed-energy  $E$  particle is most naturally expressed as a linear wave function;

$$\psi(x, t) = Ae^{i(kx-wt)} . \quad (2.3)$$

This is a wave in the positive  $x$  direction, and the wave in the opposite direction, leading to a standing wave, which is necessary to fulfill the limit conditions. This intuitively relates to our classical conception that a particle is bound up between the walls of the potential well and indicates that we choose the above wave function as the proper wave function for a momentum free- particle of  $p = \hbar k$  and energy  $E = \hbar w$ :

$$\frac{\partial^2 \psi}{\partial x^2} = -k^2 \psi. \quad (2.4)$$

It can be written as:

$$E = \frac{p^2}{2m} = \frac{\hbar^2 k^2}{2m} ; \frac{-\hbar^2}{2m} \frac{\partial^2 \psi}{\partial x^2} = \frac{p^2}{2m} \psi, \quad (2.5)$$

$$\text{similarly } \frac{\partial \psi}{\partial t} = -i\omega \psi \quad (2.6)$$

which can be written, using  $E = \omega \hbar$ , and then (2.7)

$$i\hbar \frac{\partial \psi}{\partial t} = \hbar \omega \psi = E\psi . \quad (2.8)$$

Perhaps we might extend this to the scenario where both potential energy and kinetic energy are present, then

$$E = \frac{p^2}{2m} + V(x), \quad (2.9)$$

so that

$$E\psi = \frac{p^2}{2m}\psi + V(x)\psi, \quad (2.10)$$

where wave function  $\psi$  of the motion of a particle in the presence of a potential  $V(x)$ . However, the conclusions in equations (2.5) and (2.8) still apply in this case, we can now have the equation below:

$$\frac{-\hbar^2}{2m} \frac{\partial^2 \psi}{\partial x^2} + V(x)\psi = i\hbar \frac{\partial \psi}{\partial t} \quad (2.11)$$

which is known as the time-dependent Schrödinger wave equation.

### 2.2.2 The time-independent Schrodinger equation

The time dependency was incorporated via a complex exponential factor in the wave function  $e^{-iEt/\hbar}$ , we seek a solution to the wave equation of the form to extract this time dependency

$$\psi(x, t) = \psi(x)e^{-iEt/\hbar}, \quad (2.12)$$

where space and time are separately influenced by the entire wave function. This is checked if the assumption allows us to generate an equation for  $\psi(x)$ , the spatial part of the wave function.

This test solution can be replaced by the Schrödinger wave equation and the remaining partial derivatives are taken into account;

$$\frac{-\hbar^2}{2m} \frac{d^2 \psi(x)}{dx^2} e^{-iEt/\hbar} + V(x)\psi(x)e^{-iEt/\hbar} = i\hbar - e^{-iEt/\hbar} \psi(x) = E\psi(x)e^{-iEt/\hbar}. \quad (2.13)$$

We can now see that the factor  $e^{-iEt/\hbar}$  cancels from both sides of the equation, giving

$$\frac{-\hbar^2}{2m} \frac{d^2 \psi(x)}{dx^2} + V(x)\psi(x) = E\psi(x). \quad (2.14)$$

Rearranging the terms gives

$$\frac{\hbar^2}{2m} \frac{d^2\psi(x)}{dx^2} + (E - V(x))\psi(x) = 0, \quad (2.15)$$

which is the time-independent Schrödinger equation.

### 2.3 Gaps identified in the literature.

A lot of researchers have greatly worked on the radial Schrödinger equation using different methods with different potential terms. In most cases, they obtained bound state solutions (energy equation and the corresponding wave function). Some of the researchers went ahead to calculate the thermodynamic properties. Recently, few researchers have started modifying some potentials by increasing the parameters since it has been established that the more the parameters the better it fits the experimental data (Jia *et al.*, 2012). The findings of these researchers will go a long way in helping the investigation of this study.

Jia *et al.*, (2008) worked with the Asymptotic Iteration approach on the Hulthén potential. The energy value and its wave functions were achieved. The centrifugal term for large screening parameters has been employed to cope with a new approximation approach. The results were compatible with the factorisation method and supersymmetric approach.

Ikhadair, (2009) also explored Hulthen's potential utilizing Nikiforov-Uvarov. The bound state energy eigenvalues and their corresponding eigen functions were obtained. In the study, a new approximation scheme was obtained which was used for the centrifugal barrier. The approximated numerical results obtained are close to the numerical integration results that were obtained through the asymptotic iteration method.

Oyewumi *et al.*, (2013) studied the ro-vibrational energy value determined by the Shifted Deng-Fan potential model for various orbital and angular quantum states. To solve the energy eigen values and associated wave functions, the asymptotic iteration method was utilised. The thermodynamic properties were also evaluated for the Deng Shifted Fan potential. The approximate result achieved was near the exact value and its effect on the thermal parameters,

including vibration mean energy, vibrational heat capability, vibration free energy and vibrational entropy, was similar for the different molecules studied.

Liu *et al.*, (2014) used the Improved Rosen Morse potential energy model to acquire the rotational vibrational energy spectra for cesium molecule and sodium dimer. The levels of vibrational energy predicted with the use of improved Rosen Morse potential were found for cesium molecule and sodium dimer were in better agreement than the predictions by Morse potential.

Falaye *et al.*, (2014) acquired the energy eigenvalues and their corresponding eigen functions diatomic molecular potential Tietz-Wei uses the functional analysis approach, quantum mechanics supersymmetry, and asymptotic iteration technique. The results from the three methodologies were mutually compatible

Onate and Onyeaju (2017) used the approach of obtaining energy spectrum and its respective wave function utilizing the diatomic potential of Frost Musulin and also employed by the Nikiforov-Uvarov method. The author's accuracy results were checked by comparing them with the numerical results obtained from the function analysis method.

Ita *et al.*, (2017) employed the Schrödinger S-wave bounding solution by using the Nikiforov-Uvarov parametric approach to produce the generalized Woods - saxon plus Mie- type nuclear potential, the S-Wave Schrödinger equation and the energy eigen spectrum from which they obtained the energy eigenvalues and its corresponding wave function. A certain example of potential was taken into account and used to obtain another eigen spectrum. Another eigen spectrum when A, B and C are set to be equal to 0 separately in the previous energy spectrum were also obtained.

Ikot *et al.*, (2018) also used the asymptotic iteration method to obtain the energy equation and the wave function. The thermodynamic properties of Generalised molecular potential were also studied and it was stated that that the study of Generalised molecular potential is very useful for the entropy of a gaseous system.

Jia *et al.*, (2017) used different values of spectroscopic parameters were to calculate the Rydberg-Klein-Rees of six different diatomic molecules using the improved potential of Pöschl-Teller for simulating diatomic molecules by dissociating energy and equilibrium inter-nuclear distance with an average absolute deviation of less than 1 percent. It has been pointed out that the improved Pöschl -Teller potential is more in line with modelling diatomic molecules than with Morse potential since the former is a potential function of four parameters while the latter can be a potential function of three parameters because the four parameters can interact with high inter-nuclear distances.

Okorie *et al.*, (2018) using a modified factorization approach with the aid of the Pekeris approximation system, estimated the energy spectrum and associated wave function. Thermodynamic features such as vibrational mean energy, vibrational mean free energy, vibrational heat capacity and vibrational entropy of modified Yukawa potential were computed. The graph showed the different attitudes of the thermodynamic characteristics as they change with the screening parameter.

Ikot *et al.*, (2019) used the Nikiforov-Uvarov approach to research the screened kratzer potential. The ro-vibrational energy values of the Kratzer potential for lithium and hydrogen chlorides and their associated own features were resolved. It was found that the binding state energy for the distinct diatomic molecules is increasing as the orbital quantum numbers increases.

Ebomwonyi *et al.*, (2019) studied the combination of three potentials which are coulomb potential, Hulthén potential, and Pöschl -Teller potential known as Coulomb-Hulthén -Pöschl -Teller potential (CHPT) using the parametric Nikiforov-Uvarov method. The authors generated an expression for energy equation and studied the thermodynamic properties of carbon monoxide (CO). Also, the authors obtained the equation of the energy spectrum of the potential by setting A, B, and C =0 respectively. In addition, the authors calculated the information energy, Tsallis entropy, and Renyi entropy. Furthermore, the authors observed that as the temperature of the system rises, the partition function of the system increases. There is a dissociation of specific heat capacity at different values of temperature parameters.

Farout *et al.*, (2020) also used Nikiforov-Uvarov method to obtain exact solutions of Feinberg-Horodecki (FH) exact momentum states of time dependent improved deformed exponential type equation which was reduced to improved Tietz potential when some modifications are made. The eigenvalues of carbon II oxide, nitrogen dimer, hydrogen dimer and lithium hydride using spectroscopic parameters were obtained and the FH quantised eigenvalues for the same set of diatomic molecules mentioned earlier. It was observed that the diatomic molecules studied behaved differently when varied with quantised momentum, time and screening parameter.

Omugbe *et al.*, (2020) obtained the rotational-vibrational spectrum of energy, the expectation values and the thermodynamic properties were achieved in the context of the method of approximation of Wentzel- Kramers-Brillouin, which was used to obtain an improved Greene-Aldrich-based energy-spectrum, including the vibrational free energy, the vibration-free energy and the vibration entropy of Schiöberg's potential function The various values were compared and matched with the results of other results from other researchers.

Eyube *et al.*, (2020) also worked on Improved Wei potential using the exact quantization rule. The authors calculated the ro-vibrational energies of different molecules such as CO, H<sub>2</sub>, and LiH for different quantum states. The result obtained agreed with the experimental value.

Horchani *et al.*, (2020) also worked on Tietz Hua potential using the Nikiforov-Uvarov method. The ro-vibrational energy of the cesium molecule was calculated and it was shown that Tietz Hua potential fits the experiment data better than the Morse potential. It was shown that the Tietz Hua potential was one of the efficient and useful potential energy functions in fixing an experimental value for the cesium molecule and it was also stated that deformed modified Morse potential was the first most widely used potential energy function that was used for the study of interaction of diatomic molecules. But the authors noted that as the equilibrium bond length approaches 0, there is a large value rather than an infinity which leads to a small wave function for bound vibrational states. A Pekeris type approximation was utilised to solve the Schrödinger equation by means of the centrifugal term, and the theoretical values of ro-vibrational energies were compared with the experimental values. In addition, the average deviation which was calculated was less than 0.001% which made it fit for the experimental data. However, there was an observation that as average deviation was increasing, the rotational level was increasing. Another spectroscopic information about cesium dimer was recorded.

Onate *et al.*, (2021) applied the supersymmetric approach to modified Tietz-Hua potential. The authors obtained the bound state solutions and adjusted Tietz-Hua thermal characteristics. Thermal effects on hydrogen fluoride (HF), hydrogen molecule (H<sub>2</sub>) and Carbon II oxide (CO) were examined by the authors. In addition to a specific temperature range in the three molecules, the function of the vibrational partition drops exponentially at a given temperature range whereas the function of the vibration partition is constant at higher temperatures. However, the vibrational mean energy increases in an exponential order with the absolute

temperature. The vibrational specific heat capacity decreases in a monotonic manner with an increase in temperature. But as the temperature is rising, the specific heat capacity attains a constant value, the authors observed that when the temperature range is above 2, the vibrational entropy tends to be constant while the vibrational free energy decreases as the temperature is rising. The authors also compared their results with Tietz-Hua potential and it is observed that the values of the energy eigenvalues are very close.

## CHAPTER THREE

### RESEARCH METHODOLOGY

#### 3.1 Parametric Nikiforov- Uvarov Method

The parametric Nikiforov-Uvarov method was obtained from the main Nikiforov-Uvarov method by Tezcan and Sever (2008). This method is less tedious and shorter and gives an accurate result and the parametric Nikiforov-Uvarov method was obtained from the main Nikiforov-Uvarov method will be used to solve the radial Schrödinger equation for molecular attractive potential. The standard equation for the parametric Nikiforov-Uvarov method according to Tezcan and Sever (2008) is given as:

$$\left( \frac{d^2}{ds^2} + \frac{\alpha_1 - \alpha_2}{s(1 - \alpha_3 s)} \frac{d}{ds} + \frac{-\xi_1 s^2 + \xi_2 s - \xi_3}{s^2(1 - \alpha_3 s)^2} \right) \psi(s) = 0 . \quad (3.1)$$

The Schrödinger equation becomes a secondary differential equation of the form with an appropriate coordinate transformation which is given as:

$$\frac{d^2 \psi(s)}{ds^2} + \frac{\tilde{\tau}(s)}{\sigma(s)} \frac{d\psi(s)}{ds} + \frac{\tilde{\sigma}(s)}{\sigma^2} \psi(s) = 0, \quad (3.2)$$

where  $\sigma(s)$ ,  $\tilde{\sigma}(s)$  are polynomials at the most second degree and  $\tilde{\tau}(s)$  is a first-degree polynomial. In this method, we define

$$\pi(s) = \frac{(\sigma' - \tilde{\tau})}{2} \pm \sqrt{\left( \frac{\sigma' - \tilde{\tau}}{2} \right)^2 - \tilde{\sigma} + k\sigma}, \quad (3.3)$$

and

$$\lambda = k + \pi'(s), \quad (3.4)$$

where  $\lambda$  and  $k$  are constants. Since square root under the square of the polynomial  $\pi$  in equation (3.3) must be a polynomial, which defines the constant  $k$  by putting  $k$  into equation (3.3), we have

$$\tau(s) = \tilde{\tau}(s) + 2\pi(s). \quad (3.5)$$

Since  $\rho(s) > 0$  and  $\sigma(s) > 0$ , then the derivative of  $\tau$  will be negative Nikiforov and Uvarov (1988). This provides the choice of the solution. If  $\lambda$  in equation (3.4) is:

$$\lambda = \lambda_n = -n\tau' - \frac{[n(n-1)\sigma']}{2}, n = 0,1,2, \dots \quad (3.6)$$

The hypergeometric equation has a particular grade  $n$  solution of equation (3.1) with two independent parts can be attained

$$\psi(s) = \phi(s) y(s), \quad (3.7)$$

where  $y(s)$  can be given as:

$$y_n(s) = \frac{B_n}{\rho(s)} \frac{d^n}{ds^n} [\sigma^n(s) \rho(s)] \quad (3.8)$$

and  $\rho(s)$  should satisfy the condition:

$$\frac{d}{ds} [\rho(s)\sigma(s)] = \tau(s) \rho(s), \quad (3.9)$$

the other factor can be written as:

$$\frac{\phi'(s)}{\phi(s)} = \frac{\pi(s)}{\sigma(s)}. \quad (3.10)$$

The typical structure of the Schrödinger equation, which is accessible with many potentials;

$$\left( \frac{d^2}{ds^2} + \frac{\alpha_1 - \alpha_2}{s(1 - \alpha_3 s)} \frac{d}{ds} + \frac{-\xi_1 s^2 + \xi_2 s - \xi_3}{s^2(1 - \alpha_3 s)^2} \right) \psi(s) = 0. \quad (3.11)$$

We may solve this as follows. When equation (3.11) is compared with equation (3.2), we have;

$$\tilde{\tau} = \alpha_1 - \alpha_2 s, \quad (3.12)$$

and

$$\sigma = s(1 - \alpha_3 s). \quad (3.13)$$

Also

$$\tilde{\sigma} = -\xi_1 s^2 + \xi_2 s - \xi_3. \quad (3.14)$$

Substituting equations (3.12), (3.13), and (3.14) into equation (3.3) yields:

$$\pi = \alpha_4 + \alpha_5 s \pm \sqrt{(\alpha_6 - k\alpha_3)s^2 + (\alpha_7 + k)s + \alpha_8}, \quad (3.15)$$

according to Tezcan and Sever (2008)

$$\alpha_4 = \frac{1-\alpha_1}{2}, \quad (3.16)$$

$$\alpha_5 = \frac{\alpha_2 - 2\alpha_3}{2}, \quad (3.17)$$

$$\alpha_6 = \alpha_5^2 + \xi_1, \quad (3.18)$$

$$\alpha_7 = 2\alpha_4\alpha_5 - \xi_2, \quad (3.19)$$

$$\alpha_8 = \alpha_4^2 + \xi_3. \quad (3.20)$$

The function under square root must be the square of a polynomial in equation (3.15)

according to Nikiforov and Uvarov method, so that

$$k_{1,2} = -(\alpha_7 + 2\alpha_3\alpha_8) \pm 2\sqrt{\alpha_8\alpha_9}; \quad (3.21)$$

where we define

$$\alpha_9 = \alpha_3\alpha_7 + \alpha_3^2\alpha_8 + \alpha_6, \quad (3.22)$$

for each k the following  $\pi$ 's are obtained. For

$$k = -(\alpha_7 + 2\alpha_3\alpha_8) - 2\sqrt{\alpha_8\alpha_9} \quad (3.23)$$

$\pi$  can now be written as

$$\pi = \alpha_4 + \alpha_5 s - [(\sqrt{\alpha_9} + \alpha_3\sqrt{\alpha_8})s - \sqrt{\alpha_8}], \quad (3.24)$$

for the same k, from equation (3.4), equation (3.12) and equation (3.15)

$$\tau = \alpha_1 + 2\alpha_4 - (\alpha_2 - 2\alpha_5)s - 2[(\alpha_3\sqrt{\alpha_8} + \sqrt{\alpha_9})s - \sqrt{\alpha_8}] \quad (3.25)$$

and

$$\begin{aligned} \tau' &= -(\alpha_2 - 2\alpha_5) - 2(\alpha_3\sqrt{\alpha_8} + \sqrt{\alpha_9}), \\ &= -2\alpha_3 - 2(\alpha_3\sqrt{\alpha_8} + \sqrt{\alpha_9}) < 0, \end{aligned} \quad (3.26)$$

the following equation is calculated if equation (3.3) is combined with equation (3.25) and equation (3.26):

$$n\alpha_2 - (2n + 1)\alpha_5 + \alpha_7 + 2\alpha_3\alpha_8 + n(n - 1)\alpha_3 + (2n + 1)(\sqrt{\alpha_9} + \alpha_3\sqrt{\alpha_8}) + 2\sqrt{s\alpha_8\alpha_9} = 0, \quad (3.27)$$

which gives the equation of the energy spectrum of a given problem. From equation (3.9)

$$\rho(s) = s^{\alpha_{10}-1}(1 - \alpha_3s)^{\frac{\alpha_{11}}{\alpha_3}-\alpha_{10}-1}, \quad (3.28)$$

is found and when this is used in equation (3.7)

$$y_n = P_n^{(\alpha_{10}-1, \frac{\alpha_{11}}{\alpha_3}-\alpha_{10}-1)}(1 - 2\alpha_3s), \quad (3.29)$$

is obtained, where:

$$\alpha_{10} = \alpha_1 + 2\alpha_4 + 2\sqrt{\alpha_8} \quad (3.30)$$

and

$$\alpha_{11} = \alpha_2 - 2\alpha_5 + 2(\alpha_3\sqrt{\alpha_8} + \sqrt{\alpha_9}) \quad (3.31)$$

and Jacobi polynomials are  $P_n^{(\alpha, \beta)}$  using equation (3.9)

$$\phi(s) = s^{\alpha_{12}}(1 - \alpha_3s)^{-\alpha_{12}-\frac{\alpha_{13}}{\alpha_3}} \quad (3.32)$$

is achieved and the general solution will be written as

$$\psi = \phi(s)y(s), \quad (3.33)$$

$$\psi = s^{\alpha_{12}}(1 - \alpha_3s)^{-\alpha_{12}-\frac{\alpha_{13}}{\alpha_3}} P_n^{(\alpha_{10}-1, \frac{\alpha_{11}}{\alpha_3}-\alpha_{10}-1)}(1 - 2\alpha_3s). \quad (3.34)$$

Alpha functions here are given by

$$\alpha_{12} = \alpha_4 + \sqrt{\alpha_8} \quad (3.35)$$

and

$$\alpha_{13} = \alpha_5 - (\sqrt{\alpha_9} + \alpha_3\sqrt{\alpha_8}) \quad (3.36)$$

$\alpha_3 = 0$  in some problems. For this type of problems when

$$\lim_{\alpha_3 \rightarrow 0} P_n^{(\alpha_{10}-1, \frac{\alpha_{11}}{\alpha_3}-\alpha_{10}-1)}(1 - \alpha_3s) = L_n^{\alpha_{10}-1}(\alpha_{11}s) \quad (3.37)$$

and

$$\lim_{\alpha_3 \rightarrow 0} (1 - \alpha_3s)^{-\alpha_{12}-\frac{\alpha_{13}}{\alpha_3}} = e^{\alpha_{13}s}. \quad (3.38)$$

The solution in equation (3.34) can be written as:

$$\psi = s^{\alpha_{12}} e^{\alpha_{13}s} L_n^{\alpha_{10}-1}(\alpha_{11}s), \quad (3.39)$$

one may need a second solution of equation (3.10) in some cases, but in this case, the same procedure is followed by using:

$$k = -(\alpha_7 + 2\alpha_3\alpha_8) + 2\sqrt{\alpha_8\alpha_9} \quad (3.40)$$

and the solution obtained as:

$$\psi = s^{\alpha_{12}^*} (1 - \alpha_3 s)^{-\alpha_{12}^* - \frac{\alpha_{13}^*}{\alpha_3}} P_n^{\left(\alpha_{10}^* - 1, \frac{\alpha_{11}^*}{\alpha_3} - \alpha_{10}^* - 1\right)} (1 - 2\alpha_3 s) \quad (3.41)$$

and the energy spectrum is

$$\begin{aligned} \alpha_2 n - 2\alpha_5 n + (2n + 1)(\sqrt{\alpha_9} - \alpha_3\sqrt{\alpha_8}) + n(n - 1)\alpha_3 \\ + \alpha_7 + 2\alpha_3\alpha_8 - 2\sqrt{\alpha_8\alpha_9} + \alpha_5 = 0. \end{aligned} \quad (3.42)$$

Pre-defined  $\alpha$  parameters are;

$$\begin{aligned} \alpha_{10}^* &= \alpha_1 + 2\alpha_4 - 2\sqrt{\alpha_8}, \\ \alpha_{11}^* &= \alpha_2 - 2\alpha_5 + 2(\sqrt{\alpha_9} - \alpha_3\sqrt{\alpha_8}), \\ \alpha_{12}^* &= \alpha_4 - \sqrt{\alpha_8}, \\ \alpha_{13}^* &= \alpha_5 - (\sqrt{\alpha_9} - \alpha_3\sqrt{\alpha_8}). \end{aligned} \quad (3.43)$$

### 3.2 Solution of radial Schrödinger equation.

Many of the potentials utilised in conjunction with the Schrödinger equation are the main potentials which depend on a separation between a particle and a source point. The Schrödinger equation in spherical coordinate by Pahlavani (2012) which is written as

$$\left\{ \frac{-\hbar^2}{2\mu} \left[ \frac{1}{r^2} \frac{\partial}{\partial r} \left( r^2 \frac{\partial}{\partial r} \right) + \frac{1}{r^2 \sin\theta} \frac{\partial}{\partial \theta} \left( \sin\theta \frac{\partial}{\partial \theta} \right) + \frac{1}{r^2 \sin^2\theta} \frac{\partial^2}{\partial \phi^2} \right] + V(r) \right\} \psi(r, \theta, \phi) = E\psi(r, \theta, \phi), \quad (3.44)$$

can be explained as the distance  $r$  from the origin of the coordinate system and two angles is defined as a point in space, Zenith angle  $\theta$  and azimuthal angle  $\phi$ . Therefore, to use these triplets  $(r, \theta, \phi)$ , we can express a particular point in three-dimensional space. A unique set of

spherical coordinates can be defined for each point, the range can be in the form  $r \geq 0, 0 \leq \theta \leq \pi$  and  $0 \leq \phi \leq 2\pi$ .

The Schrödinger equation in spherical coordinate can be solved by using the separation of the wave function in terms of independent wave functions i.e.  $\psi(r, \theta, \phi) = R(r)Y(\theta, \phi)$ . The rotation of a molecule or the movement of an electron through an atomic nucleus could be described in spherical coordinate by making use of a single coordinate i.e. the Coulomb potential that describes the electromagnetic interaction between an electron and a portion can be written as  $V(x,y,z) = \frac{e^1}{\sqrt{x^2+y^2+z^2}}$  in Cartesian coordinates, where  $e^1 = \frac{e}{\sqrt{4\pi\epsilon_0}}$ ,  $e$  is the elementary electric charge and  $\epsilon_0$  is the electric permittivity of free space. It might not be straightforward to solve the Schrödinger equation with the potential  $V(x,y,z)$  because the potential has three variables that are not separable in Cartesian coordinates, therefore the potential would be turned to  $V(r) = \frac{-e^1}{r}$  which depend only on  $r$ . for this transformation, we used the conversion  $r = \sqrt{x^2 + y^2 + z^2}$ . The variables  $(x,y,z)$  in Cartesian coordinate could be connected to the variables  $(r, \theta, \phi)$  in spherical coordinate, as follows:

$$X = r \sin \theta \cos \phi, y = r \sin \theta \sin \phi, z = r \cos \theta,$$

$$\theta = \cos^{-1} \left( \frac{z}{r} \right), \phi = \tan^{-1} \left( \frac{y}{x} \right). \quad (3.45)$$

The separable variables in spherical coordinates can be achieved using the relation of  $\nabla^2$  in spherical coordinate as we derive the Schrödinger equation in the same coordinate. So, the Schrödinger equation is written as equation 3.44,

where the  $\nabla^2$  is given in spherical coordinates:

$$\nabla^2 = \frac{1}{r^2} \frac{\partial}{\partial r} \left( r^2 \frac{\partial}{\partial r} \right) + \frac{1}{r^2 \sin \theta} \frac{\partial}{\partial \theta} \left( \sin \theta \frac{\partial}{\partial \theta} \right) + \frac{1}{r^2 \sin^2 \theta} \frac{\partial^2}{\partial \phi^2}. \quad (3.46)$$

The potential we are interested in is central because it only depends on the distance  $r$  from the origin and we look for a separable solution of the Schrödinger equation

$$\psi(r, \theta, \phi) = R(r)Y(\theta, \phi), \quad (3.47)$$

using the assumed form of  $\psi(r, \theta, \phi)$  we may write the Schrödinger equation as:

$$\frac{1}{R(r)} \frac{d}{dr} \left( r^2 \frac{dR(r)}{dr} \right) + \frac{2\mu}{\hbar^2} r^2 (E - V(r)) R(r) = \frac{1}{Y(\theta, \phi)} \left[ \frac{1}{\sin\theta} \frac{\partial}{\partial\theta} \left( \sin\theta \frac{\partial Y(\theta, \phi)}{\partial\theta} \right) + \frac{1}{\sin^2\theta} \frac{\partial^2 Y(\theta, \phi)}{\partial\phi^2} \right]. \quad (3.48)$$

The expressions on both sides of the equation (3.48) are equivalent if they are the same as a constant  $L$ , where  $L = \ell(\ell + 1)$ . The next two equations must therefore be true at the same time:

$$\frac{1}{r^2} \frac{d}{dr} \left( r^2 \frac{dR(r)}{dr} \right) + \left[ \frac{2\mu}{\hbar^2} (E - V(r)) - \frac{L}{r^2} \right] R(r) = 0 \quad (3.49)$$

and

$$\frac{1}{\sin\theta} \frac{\partial}{\partial\theta} \left( \sin\theta \frac{\partial Y(\theta, \phi)}{\partial\theta} \right) + \frac{1}{\sin^2\theta} \frac{\partial^2 Y(\theta, \phi)}{\partial\phi^2} + LY(\theta, \phi) = 0. \quad (3.50)$$

Then, we have two independent equations and we can deal with these individually because the equation is made up of solely radial variables in equation (3.49) and equation (3.50). The Schrödinger wave equation is given as:

$$\frac{d^2\psi(r)}{dr^2} + \frac{2\mu}{\hbar^2} \left[ E - V(r) - \hbar^2 \frac{l(l+1)}{2\mu r^2} \right] \psi(r) = 0. \quad (3.51)$$

The attractive potential formulated by Williams and Poullos (1993) is given as:

$$V(r) = \frac{Ae^{-2\alpha r} + Be^{-\alpha r} + C}{(1 - e^{-\alpha r})^2}, \quad (3.52)$$

where  $D_e$ ,  $e^{\alpha r_e}$  and  $e^{2\alpha r_e}$  are used to modify the molecular attractive potential which is now given as:

$$V(r) = D_e \left[ \frac{Ae^{2\alpha r_e} + Be^{\alpha(r+r_e)} + Ce^{2\alpha r}}{(1 - e^{-\alpha r})^2} \right] e^{-2\alpha r}, \quad (3.53).$$

where

$V(r)$  is the interacting potential,

$D_e$  is the dissociation energy,

$r_e$  is the equilibrium bond length,

$\alpha$  is the screening parameter,

$E$  is the non relativistic energy of the system,

$\mu$  is the reduced mass ,

$\hbar$  is the reduced Planck's constant,

$n$  is the principal quantum number,

$R_{n\ell}(r)$  is the wave function,

A, B and C are the potential strengths,

$\ell$  is the orbital angular momentum quantum number.

Substituting equation (3.53) into equation (3.52) gives:

$$\frac{d^2\psi(r)}{dr^2} + \frac{2\mu E}{\hbar^2} - \frac{2\mu}{\hbar^2} \left[ D_e \left[ \frac{Ae^{2\alpha r_e} + Be^{\alpha(r+r_e)} + Ce^{2\alpha r}}{(1-e^{-\alpha r})^2} \right] e^{-2\alpha r} \right] - l(l+1) \frac{\alpha^2 e^{-\alpha r}}{(1-e^{-\alpha r})^2} = 0. \quad (3.54)$$

Defining a simple variable of the form  $y = e^{-\alpha r}$  and substituting it into equation (3.54) leads to the equation of the form:

$$\frac{\frac{d^2}{dy^2} + \frac{1}{y} \frac{d}{dy} - (\varepsilon A e^{2\alpha r_e} - \delta_o) y^2 + (-2\delta_o - \varepsilon B e^{\alpha r_e} - l(l+1)y) - (\varepsilon C - \delta_o)}{y^2(1-y)^2} = 0, \quad (3.55)$$

$$\text{where } \delta_o = \frac{2\mu E}{\alpha^2 \hbar^2} \quad \text{and } \varepsilon = \frac{2\mu D_e}{\alpha^2 \hbar^2}$$

$$(\varepsilon C - \delta_o) = 0, \quad (3.56)$$

$$(\varepsilon C - \delta_o) = 0 , \quad (3.57)$$

$$\alpha_1 = \alpha_2 = \alpha_3 = 1 , \quad (3.58)$$

$$\alpha_4 = 0 , \quad (3.59)$$

$$\alpha_5 = \frac{\alpha_2 - 2\alpha_3}{2} = \frac{1-2}{2} = \frac{-1}{2} , \quad (3.60)$$

$$\alpha_6 = \frac{1}{4} - \delta_o + \varepsilon A e^{2\alpha r_e} , \quad (3.61)$$

$$\alpha_7 = 2\delta_o + \varepsilon B e^{\alpha r_e} + l(l+1) , \quad (3.62)$$

$$\alpha_8 = \varepsilon C - \delta_o , \quad (3.63)$$

$$\alpha_9 = \frac{1}{4} + \varepsilon (A e^{2\alpha r_e} + B e^{\alpha r_e} + C) + l(l+1) , \quad (3.64)$$

$$\alpha_{10} = 1 + 2\sqrt{\varepsilon C - \delta_o} , \quad (3.65)$$

$$\alpha_{11} = 2\left(1 + \sqrt{\varepsilon C - \delta_o}\right) + \sqrt{4\varepsilon(A e^{2\alpha r_e} + B e^{\alpha r_e} + C) + (1+2l)^2} , \quad (3.66)$$

$$\alpha_{12} = \sqrt{\varepsilon C - \delta_o} , \quad (3.67)$$

$$\alpha_{13} = -\frac{1}{2} - \frac{1}{2}\sqrt{4\varepsilon(A e^{2\alpha r_e} + B e^{\alpha r_e} + C) + (1+2l)^2} - \sqrt{\varepsilon C - \delta_o} . \quad (3.68)$$

Substitute equation (3.58) to equation (3.64) into equation (3.27) yields the equation's energy and the corresponding wave equation which is expressed as;

$$E_{n,\ell} = C D_e - \frac{\alpha^2 h^2}{2\mu} \left[ \frac{\varepsilon(2C + B e^{\alpha r_e}) + \ell(\ell+1) + n(n+1) + \left(n + \frac{1}{2}\right)\vartheta + \frac{1}{2}}{1+2n+\vartheta} \right]^2 , \quad (3.69)$$

$$R_{n,\ell}(y) = y^\chi (1-y)^{\frac{1}{2}(1+\vartheta)} \times P_n^{(2\chi, \vartheta)}(1-2y) , \quad (3.70)$$

where

$$\chi = \sqrt{\varepsilon C - \frac{2\mu E_{n,\ell}}{\alpha^2 h^2}} , \quad (3.71)$$

$$\vartheta = \sqrt{4\varepsilon(A e^{2\alpha r_e} + B e^{\alpha r_e} + C) + (1+2\ell)^2} . \quad (3.72)$$

### 3.3 The Molecular Attractive Potential and Thermodynamic Properties

Thermodynamics is the study of how heat and energy relate when mechanical work is produced from the system. The thermodynamics properties that will be considered in this thesis are as

follows: vibrational partition function, vibrational mean energy, vibrational specific heat capacity, vibrational entropy and vibrational free energy.

The vibrational partition function serves as the starting point for the determination of other thermodynamic properties of a system. To get the vibrational partition function of a system, all the available vibrational energy levels of the system are added directly Okorie *et al.*, (2018). It depicts the number of microstates that is accessible to a system in a given ensemble.

The energy equation given in equation (3.27) is stated in a concise manner to determine the thermodynamic parameters for the molecular attractive potential.

$$E_n = - \left[ Q_2 \rho^2 + \frac{Q_2 Q_3^2}{\rho^2} \right] + Q_1 - 2Q_1 Q_3, \quad (3.73)$$

$$\left. \begin{aligned} Q_1 &= D_e \delta = \frac{1}{2} + \frac{1}{2} \sqrt{1 + 4\epsilon(Ae^{2are} + Be^{are} + C)}, \\ Q_2 &= \frac{\alpha^2 \hbar^2}{8\mu}, \\ Q_3 &= -\epsilon A e^{2are}. \end{aligned} \right\} \quad (3.74)$$

After the energy equation is expressed in a compact form which allows thermodynamic properties to be calculated, the system partition function can be defined as:

$$z = \int_0^\lambda e^{-\beta E_n} dn. \quad (3.75)$$

where  $\beta = (k_B T)^{-1}$  with  $k_B$  being the Boltzmann constant.

Now, defining  $\rho = (n + \delta)$  and substituting equation (3.73) into equation (3.75), the above-mentioned partition function can be written as:

$$z = e^{\beta(2Q_1 Q_3 - Q_1)} \int_0^\lambda e^{\beta \left( Q_2 \rho^2 + \frac{Q_2 Q_3^2}{\rho^2} \right)} d\rho \quad (3.76)$$

The partition function of equation (3.76) is used with Mathematical 10.0 version to have:

$$Z(\beta) = \frac{e^{\chi_1[e^{-\chi_2(1+\chi_4)}+e^{\chi_3(-1+\chi_5)}]}}{4\sqrt{-\beta Q_2}}, \quad (3.77)$$

where

$$\left. \begin{aligned} \chi_1 &= \beta(-Q_1 + 2Q_1Q_3), \\ \chi_2 &= 2\sqrt{-\beta Q_2}\sqrt{-\beta Q_2Q_3^2}, \\ \chi_3 &= -2\sqrt{-\beta Q_2}\sqrt{-\beta Q_2Q_3^2}, \\ \chi_4 &= \operatorname{erf}\left[\lambda\sqrt{-\beta Q_2} - \frac{\sqrt{-\beta Q_2Q_3^2}}{\lambda}\right], \\ \chi_5 &= \operatorname{erf}\left[\lambda\sqrt{-\beta Q_2} + \frac{\sqrt{-\beta Q_2Q_3^2}}{\lambda}\right] \end{aligned} \right\} \quad (3.78)$$

where  $\operatorname{erf}(x)$  denotes the error function which is a special function of the sigmoid shape. In Maple software the imaginary error function is given as  $\operatorname{erfi}(x)$  and can be used in many numerical calculations.

### 3.3.1 Vibrational mean energy.

With the help of the vibrational partition function of equation (3.77), we can determine the thermodynamic properties for molecular attractive potential model. The vibrational mean energy is given as:

$$\begin{aligned} U(\beta) &= -\frac{\partial \ln Z(\beta)}{\partial \beta} \\ &= U(\beta) = -\left\{ \frac{\left[ \frac{1+\chi_4+e^{2\chi_2(-1+\chi_5)}-2\beta[1+\chi_4+e^{2\chi_2(-1+\chi_5)]\Lambda_0}{\Lambda_1 4\sqrt{-\beta Q_2}[\sqrt{\pi}\beta(-1-e^{2\chi_2}-\chi_4+e^{2\chi_2}\chi_5)Q_2Q_3^2-e^{\chi_2+\Lambda_2}]} \right]}{2\beta[1+\chi_4+e^{2\chi_2(-1+\chi_5)}]} \right\}, \end{aligned} \quad (3.79)$$

where

$$\Lambda_0 = (-Q_1 + 2Q_1Q_3), \quad \Lambda_1 = \frac{1}{\sqrt{-\beta Q_2Q_3^2}\sqrt{\pi}}, \quad \Lambda_2 = \frac{\beta Q_2(\lambda^4+Q_3^2)}{\lambda^2} \lambda\sqrt{-\beta Q_2Q_3^2}. \quad (3.80)$$

### 3.3.2 Vibrational Specific heat capacity

The heat capacity is the quantities that are measured to determine the heat necessary for a certain amount to change the body's temperature. It is measured in Joules per Kelvin. The heat capacity per unit mass of a material is a special heat capacity. For certain degree of freedom, there can be no availability or only partial storage of thermal energy in a given temperature for quantum mechanical reasons. As the temperature is approaching absolute zero, the quantum mechanical effect loses the degrees of freedom available. Quantum theory can be employed in simple systems for the quantitative prediction of certain heat capacity.

$$C(\beta) = K\beta^2 \frac{\partial^2 \ln Z(\beta)}{\partial \beta^2} = \frac{\Delta_0 + \Delta_1 - 8\Delta_2 + \Delta_3}{2\pi\lambda(1 - e^{2\chi_2} + \chi_4 + e^{2\chi_2}\chi_5)^2 \Lambda_3}, \quad (3.81)$$

where

$$\Delta_0 = \pi\lambda(1 - e^{2\chi_2} + \chi_4 + e^{2\chi_2}\chi_5)^2 \Lambda_3 + 2e^{\chi_2 + \Lambda_2} \beta Q_2 \lambda^2 \left[ \frac{\sqrt{\pi} - e^{2\chi_2}\sqrt{\pi} + \sqrt{\pi} \chi_4 +}{e^{2\chi_2}\sqrt{\pi} \chi_5 + 4e^{\chi_2 + \Lambda_2} \lambda \sqrt{-\beta Q_2}} \right] \Lambda_6, \quad (3.82)$$

$$\Delta_1 = 4e^{\chi_2} \sqrt{\pi} \beta^2 Q_2^2 [-e^{\Lambda_4} \lambda^4 (1 - e^{2\chi_2} + \chi_4 + e^{2\chi_2}\chi_5)] \Lambda_6 + Q_3^2 \left( \frac{4e^{\Lambda_2} \Lambda_5 + 4e^{2\chi_2 + \Lambda_2} \Lambda_5 +}{e^{\Lambda_2} \Lambda_6 - e^{2\chi_2 + \Lambda_2} \Lambda_6} \right), \quad (3.83)$$

$$\Delta_2 = e^{\chi_2} \sqrt{\pi} \lambda \Lambda_3 \quad (3.84)$$

$$+ \Delta_4 e^{\chi_2} \chi_5 \left[ 8\sqrt{\pi} \lambda \Lambda_3 + e^{\chi_2 + \Lambda_2} \left( -4\lambda^2 \sqrt{-\beta Q_2} + \sqrt{-\beta Q_2 Q_3^2} \right) \right], \quad (3.85)$$

$$\Delta_3 = \chi_4 [-8e^{\chi_2} \sqrt{\pi} \lambda \Lambda_3 + 8e^{\chi_2} \sqrt{\pi} \lambda \Lambda_3 + e^{\Lambda_2} (4\lambda^2 \Lambda_3)], \quad (3.86)$$

$$\Lambda_3 = \sqrt{-\beta Q_2} \sqrt{-\beta Q_2 Q_3^2}, \quad (3.87)$$

$$\Lambda_4 = \frac{\beta Q_2(\lambda^4 + Q_3^2)}{\lambda^2}, \quad (3.88)$$

$$\Lambda_5 = \lambda^2 \sqrt{-\beta Q_2}, \quad (3.89)$$

$$\Lambda_6 = \sqrt{-\beta Q_2 Q_3^2}, \quad (3.90)$$

### 3.3.3 Vibrational entropy

Entropy is one of the predictors of a spontaneous reaction. The degree of disorder or unpredictability of a system is measured by entropy (S). The higher the level of a system disturbance, the larger the system entropy. Temperature influences entropy degree, noting that:

$$S = k \ln Z(\beta) - k\beta \frac{\ln Z(\beta)}{\partial \beta^2},$$

$$= k \ln \left[ \frac{e^{-\beta Q_1 + 2\beta Q_1 - \chi_2 \sqrt{\pi} [1 + \chi_4 + e^{2\chi_2} (1 + \chi_5)]}}{4\sqrt{-\beta Q_2}} \right] - K\beta \left\{ \frac{\left[ \frac{1 + \chi_4 + e^{2\chi_2} (-1 + \chi_5) - 2\beta [1 + \chi_4 + e^{2\chi_2} (-1 + \chi_5)] \Lambda_0}{4\sqrt{-\beta Q_2} (\sqrt{\pi} \beta (-1 - e^{2\chi_2} - \chi_4 + e^{2\chi_2} \chi_5) Q_2 Q_3^2 - e^{\chi_2 + \Lambda_6 \Lambda_2})} + \frac{\sqrt{\pi} \Lambda_6}{2\beta [1 + \chi_4 + e^{2\chi_2} (-1 + \chi_5)]} \right]}{2\beta [1 + \chi_4 + e^{2\chi_2} (-1 + \chi_5)]} \right\}. \quad (3.91)$$

### 3.3.4 Vibrational free energy

Free energy is a measure of the energy for activity. It is used to determine the change in systems and the extent of their work. This is a large attribute, which means the size of the substance depends upon the amount of the thermodynamic substance.

$$F(\beta) = -\frac{1}{\beta} \ln Z(\beta) = -\frac{e^{\beta \Lambda_0} \ln \sqrt{\pi} [e^{\chi_3} (1 + \chi_4) + e^{\chi_2} (\chi_5 + 1)]}{4\sqrt{-\beta Q_2}}. \quad (3.92)$$

# CHAPTER FOUR

## RESULTS, DISCUSSION OF RESULTS AND FINDINGS

The following are the results generated using MAPLE software which is used to solve issues involving linear and non - linear equations by modifying numerical methods and finding graphical solution and mathematical 10.0 version software which is used to represent, evaluate, or compute quantitative symbols.

### 4.1 Results

The graphical representation of the results generated are as follows:

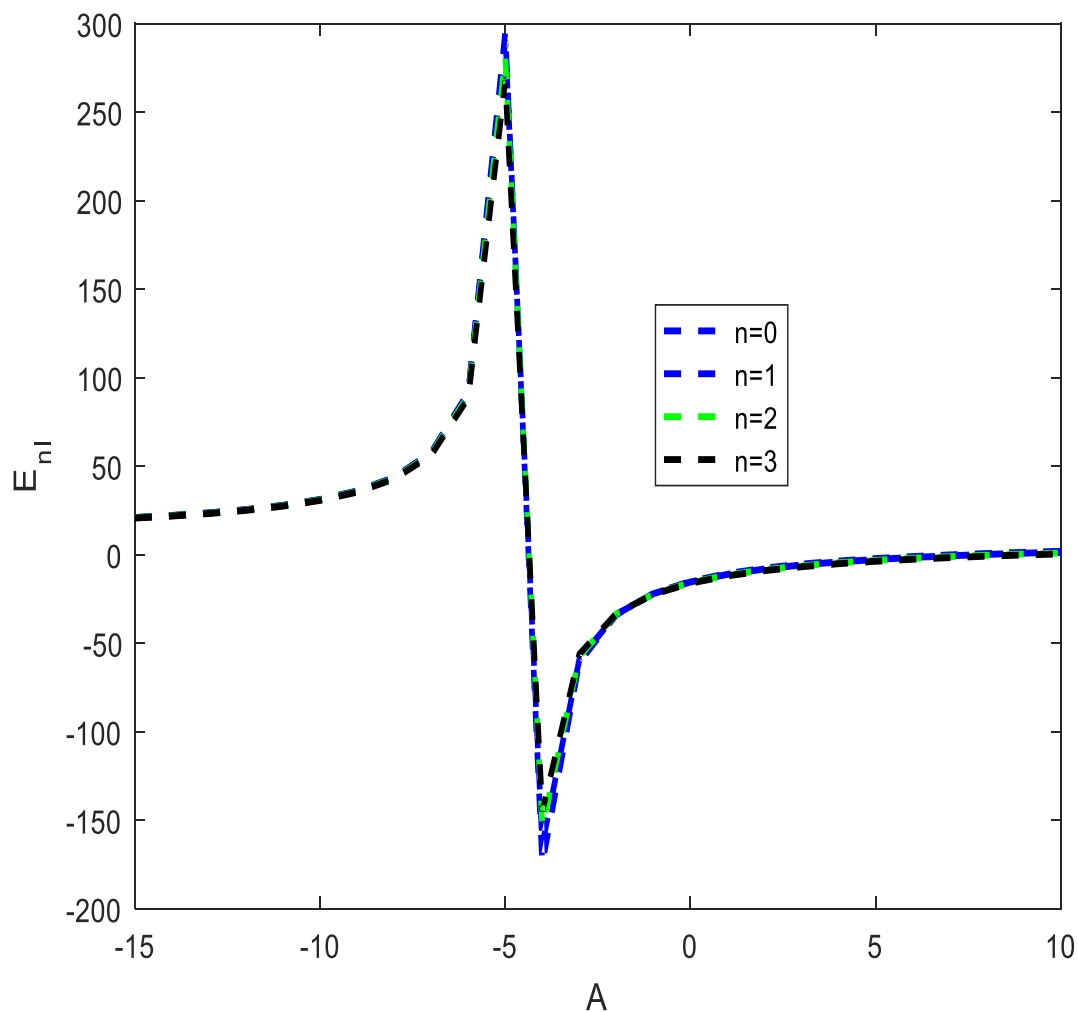


Figure 4.1: The plot of Energy (J) against potential strength A using equation (3.69)

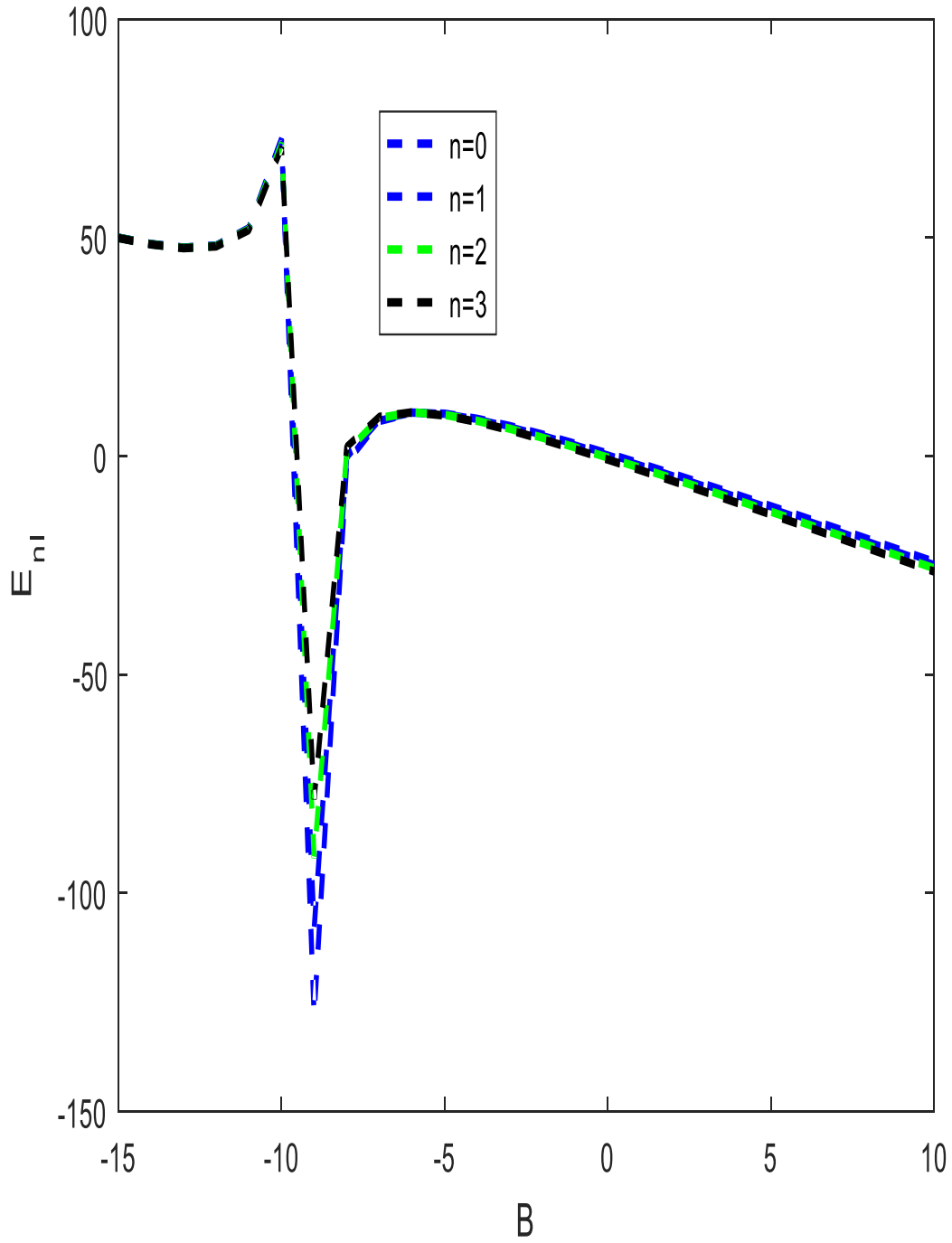


Figure 4.2: Variation of energy (J) against potential strength B using equation (3.69)

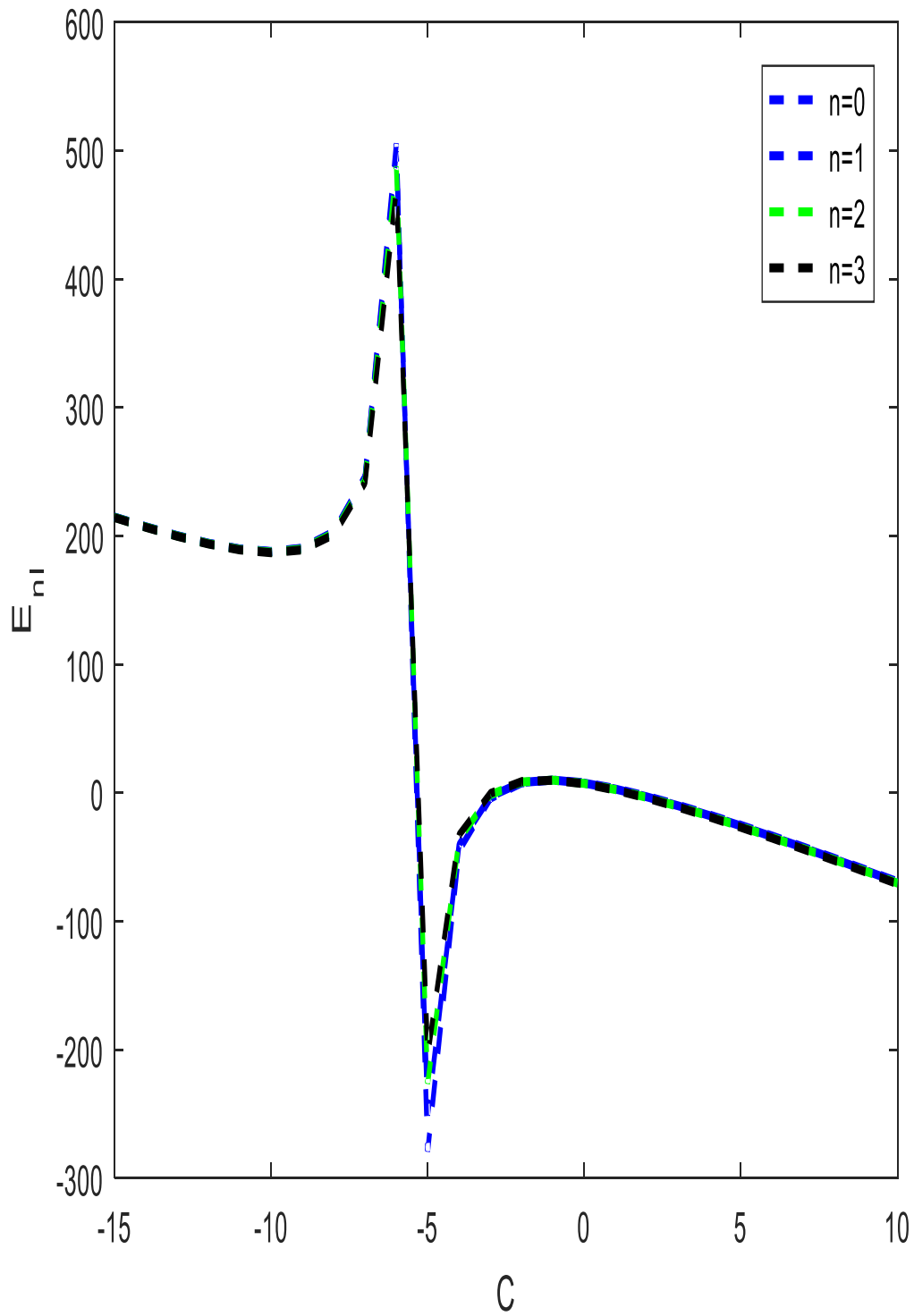


Figure 4.3: Variation of energy (J) against potential strength C using equation (3.69)

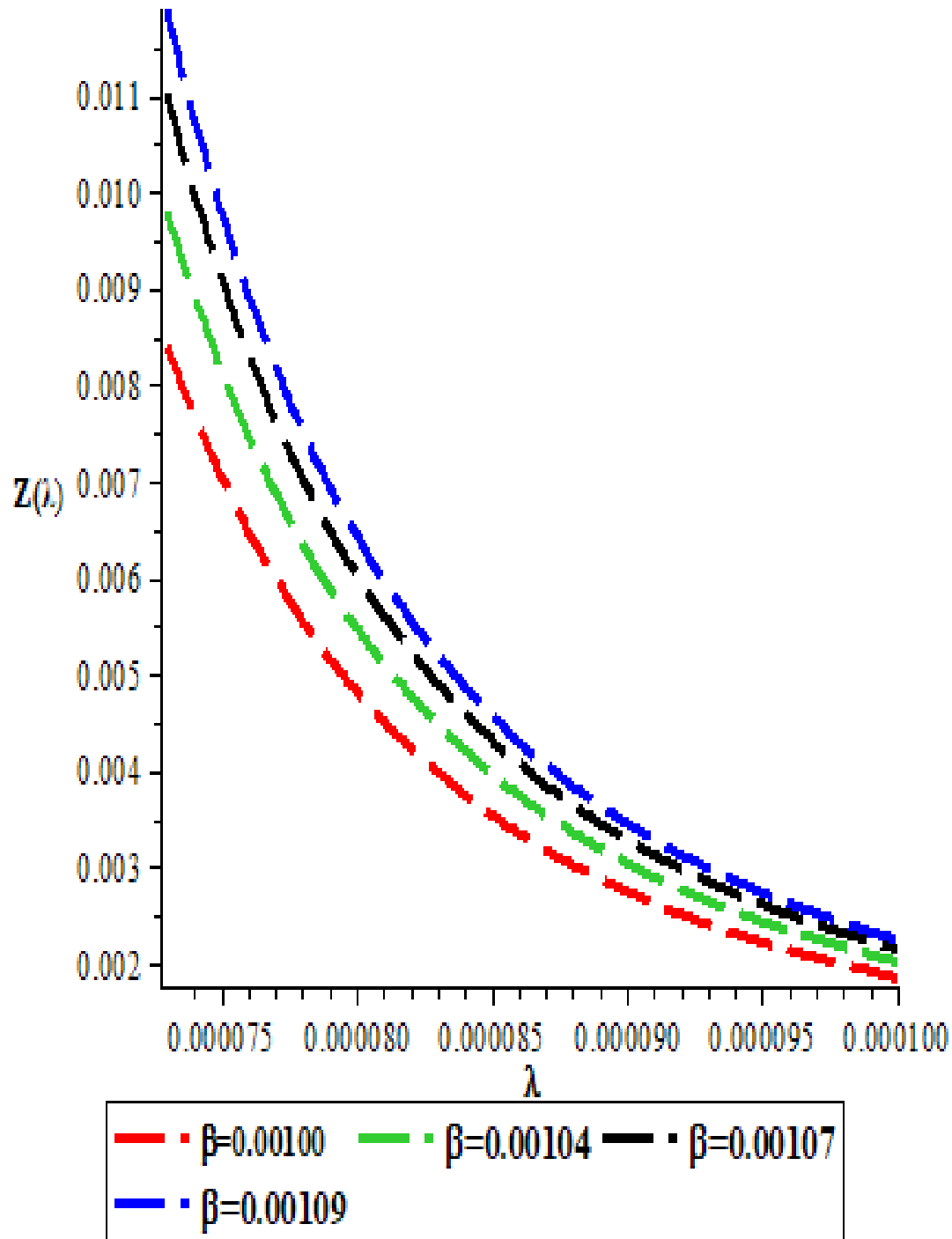


Figure 4.4: The graph of vibrational partition function versus the maximum quantum state  $\lambda$  with varying  $\beta$  using equation (3.77)

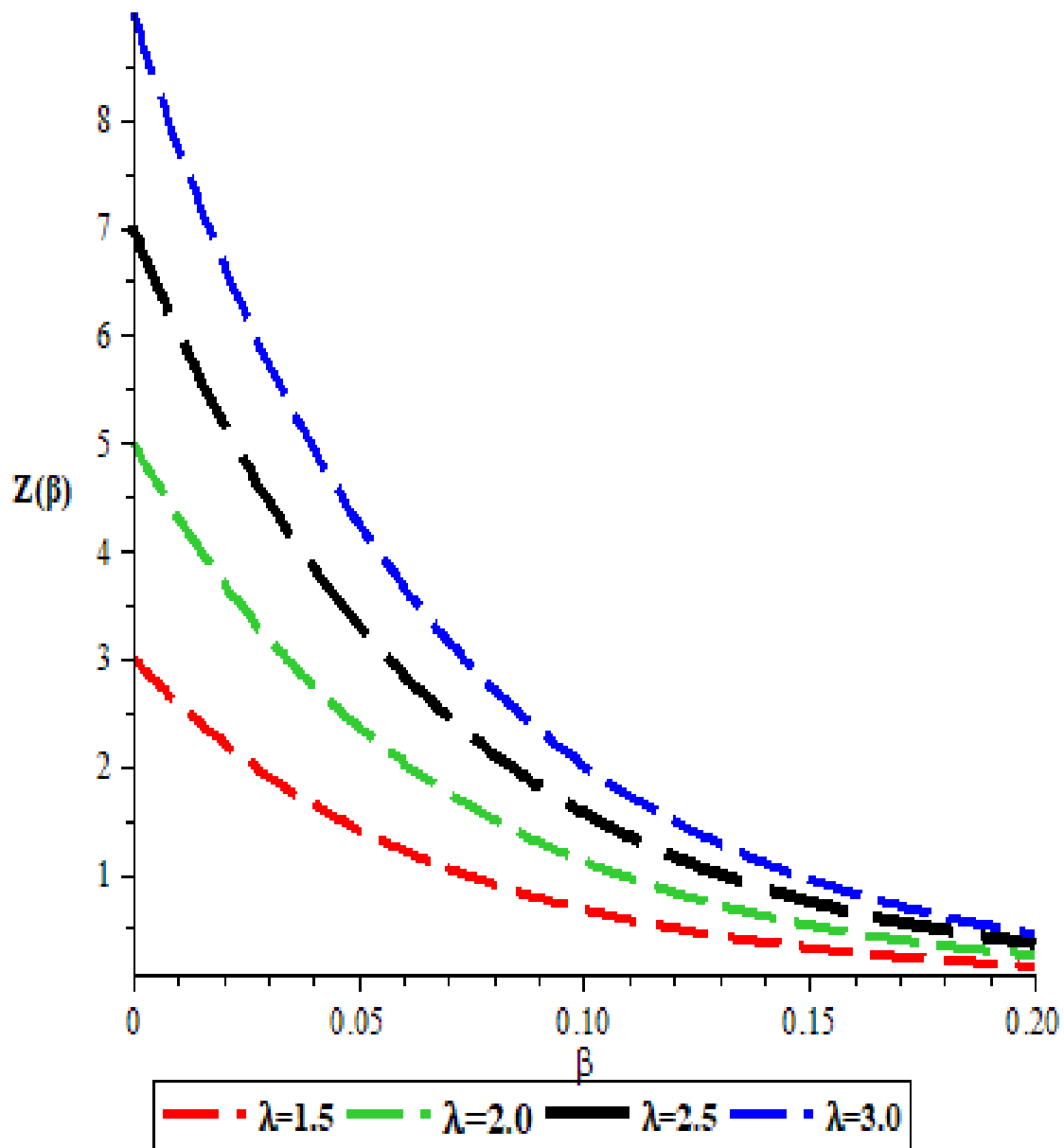


Figure 4.5: The graph of vibrational partition function versus the temperature parameter  $\beta$  with varying  $\lambda$  using equation (3.77)

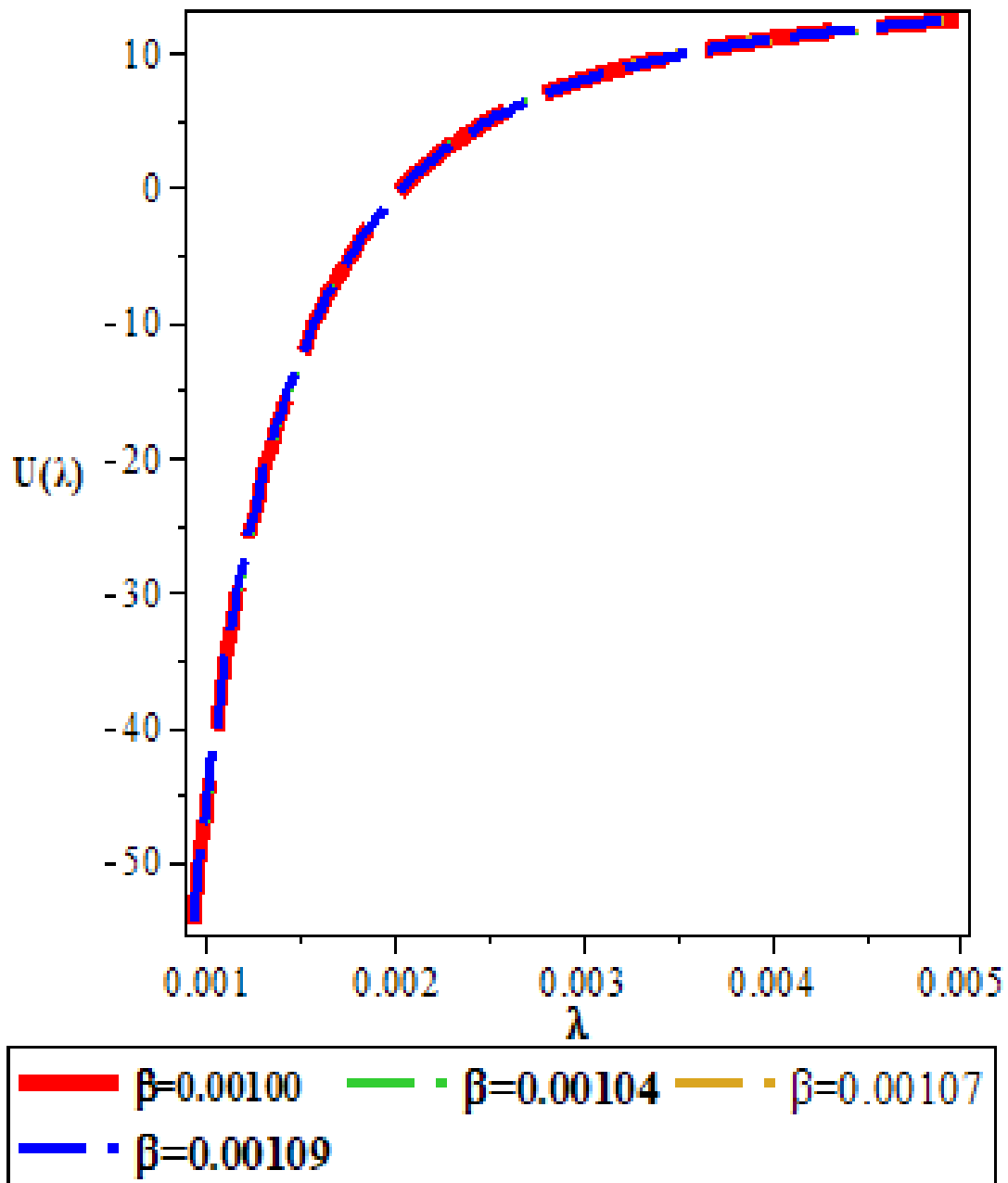


Figure 4.6: The behaviour of vibrational mean energy  $U$  (J) with the maximum quantum state  $\lambda$  with varying  $\beta$  using equation (3.79)

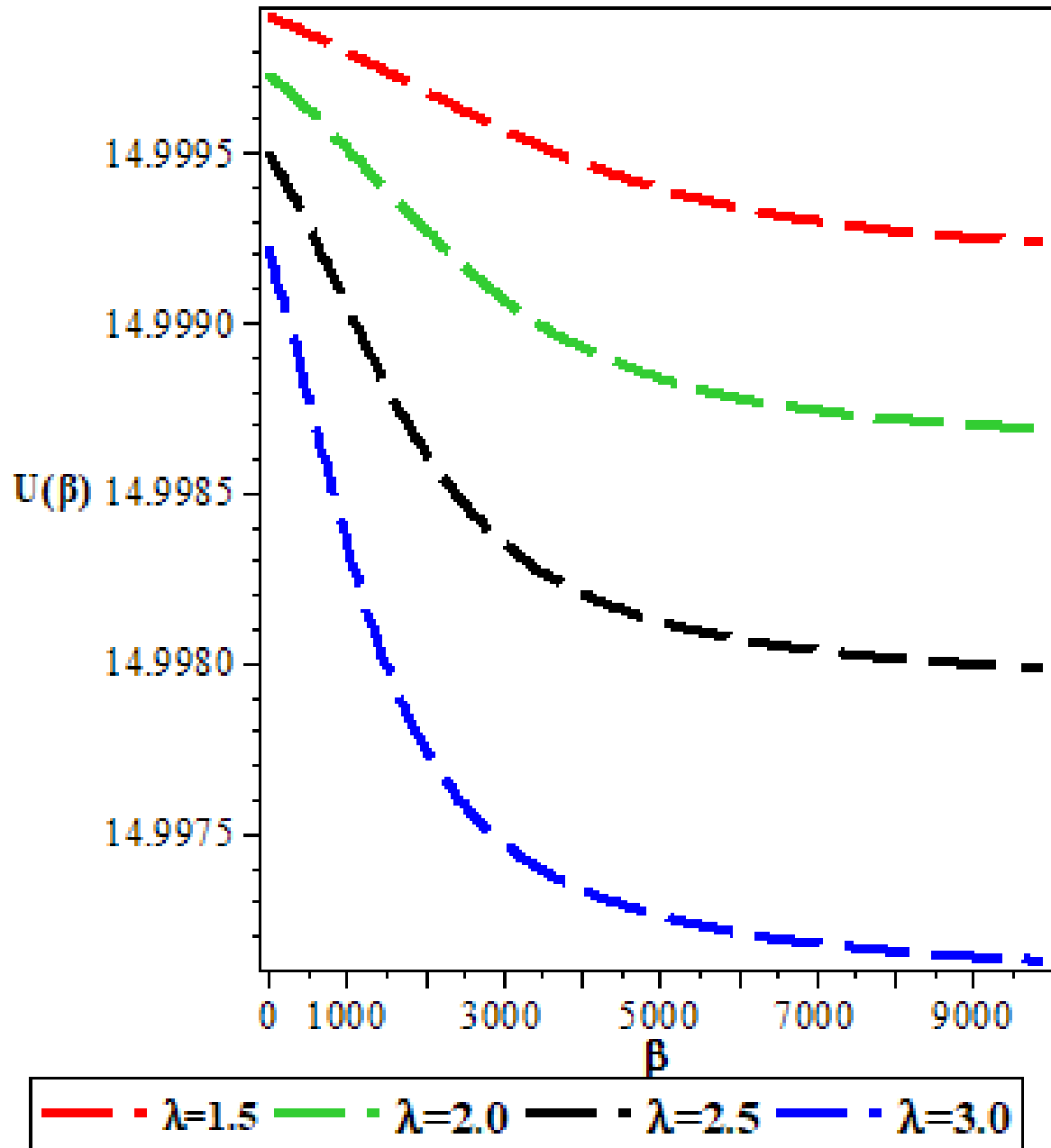


Figure 4.7: The plot of vibrational mean energy  $U$  (J) against the temperature parameter  $\beta$  with varying  $\lambda$  using equation (3.79)

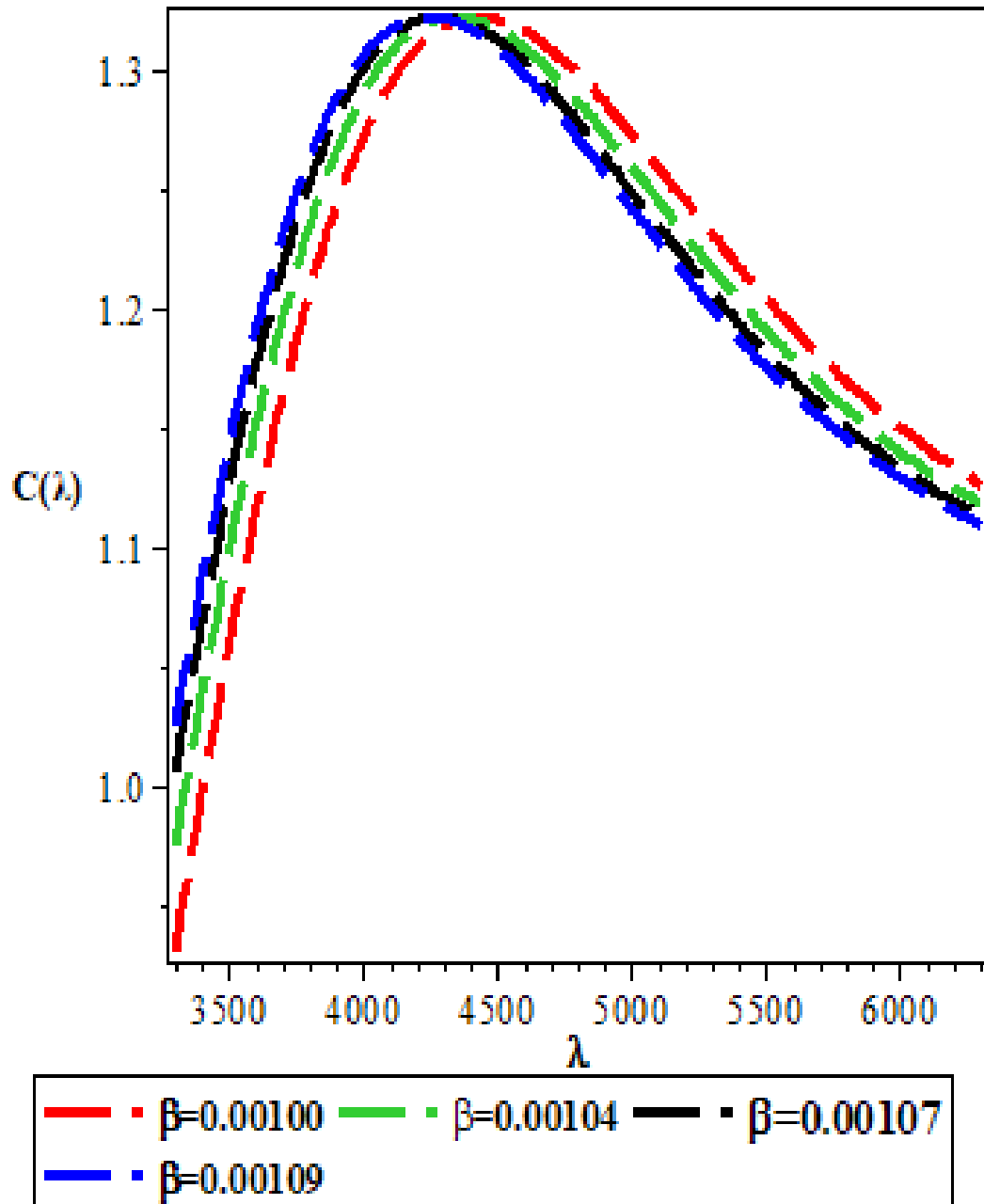


Figure 4.8: The behaviour of vibrational specific heat capacity ( $Jkg^{-1}K^{-1}$ ) against the maximum quantum state  $\lambda$  with varying  $\beta$  using equation (3.81)

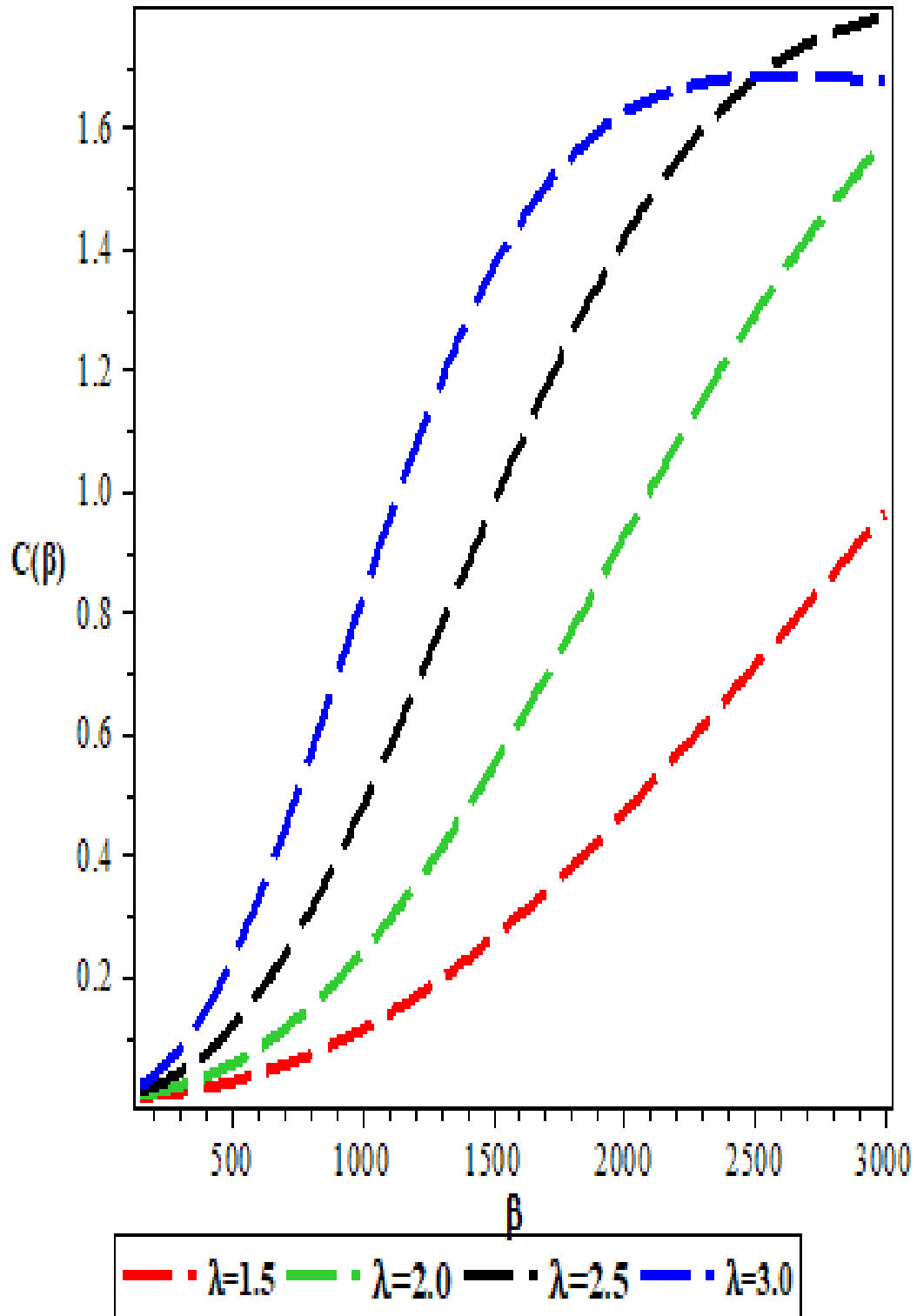


Figure 4.9: The behaviour of vibrational specific heat capacity ( $Jkg^{-1}K^{-1}$ ) against temperature parameter  $\beta$  with varying  $\lambda$  using equation (3.81)

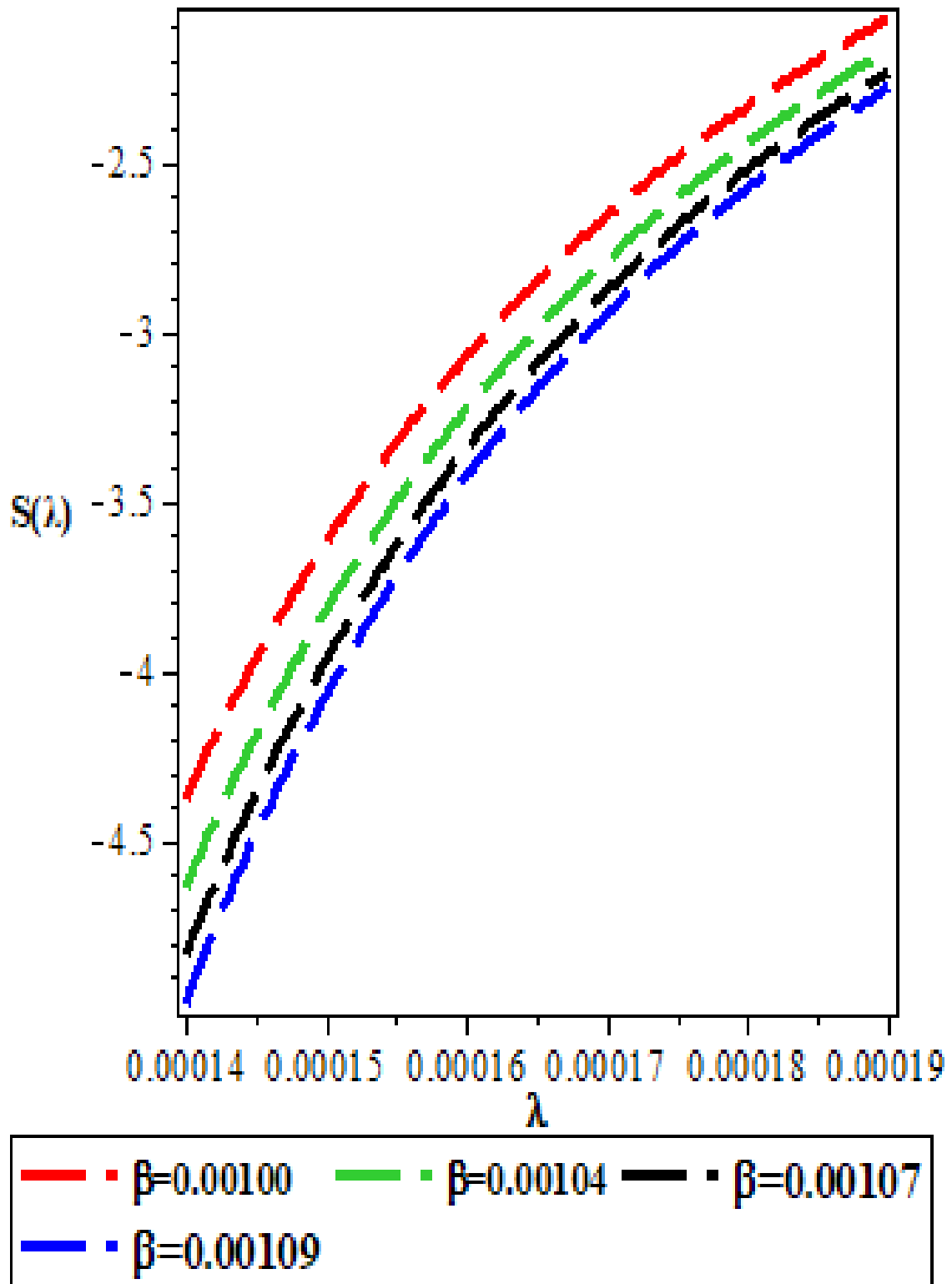


Figure 4.10: Plot of vibrational entropy ( $JK^{-1}$ ) against the maximum quantum state  $\lambda$  with varying  $\beta$  using equation (3.83)

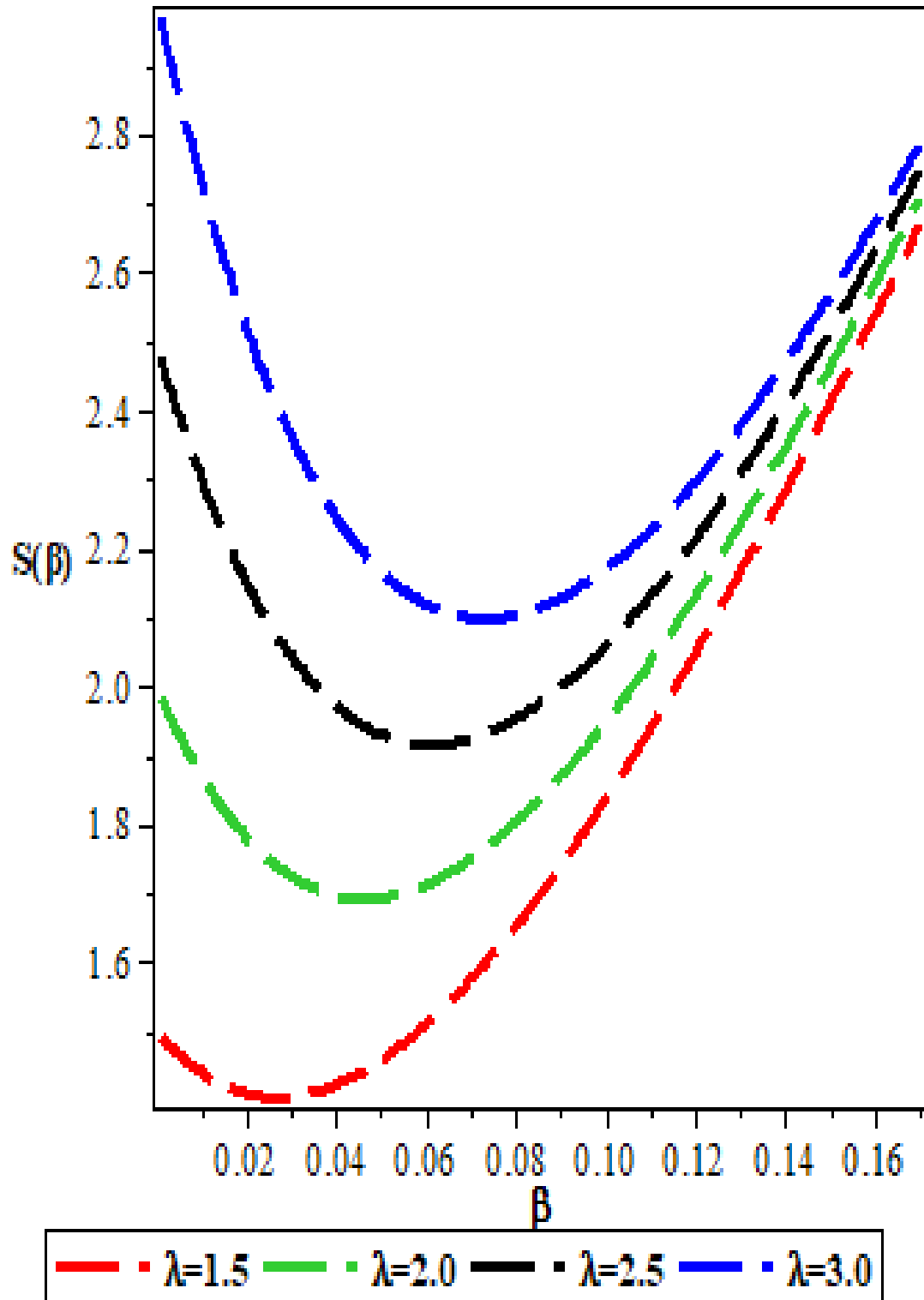


Figure 4.11: The plot of vibrational entropy ( $\text{JK}^{-1}$ ) against temperature parameter  $\beta$  with varying  $\lambda$  using equation (3.83)

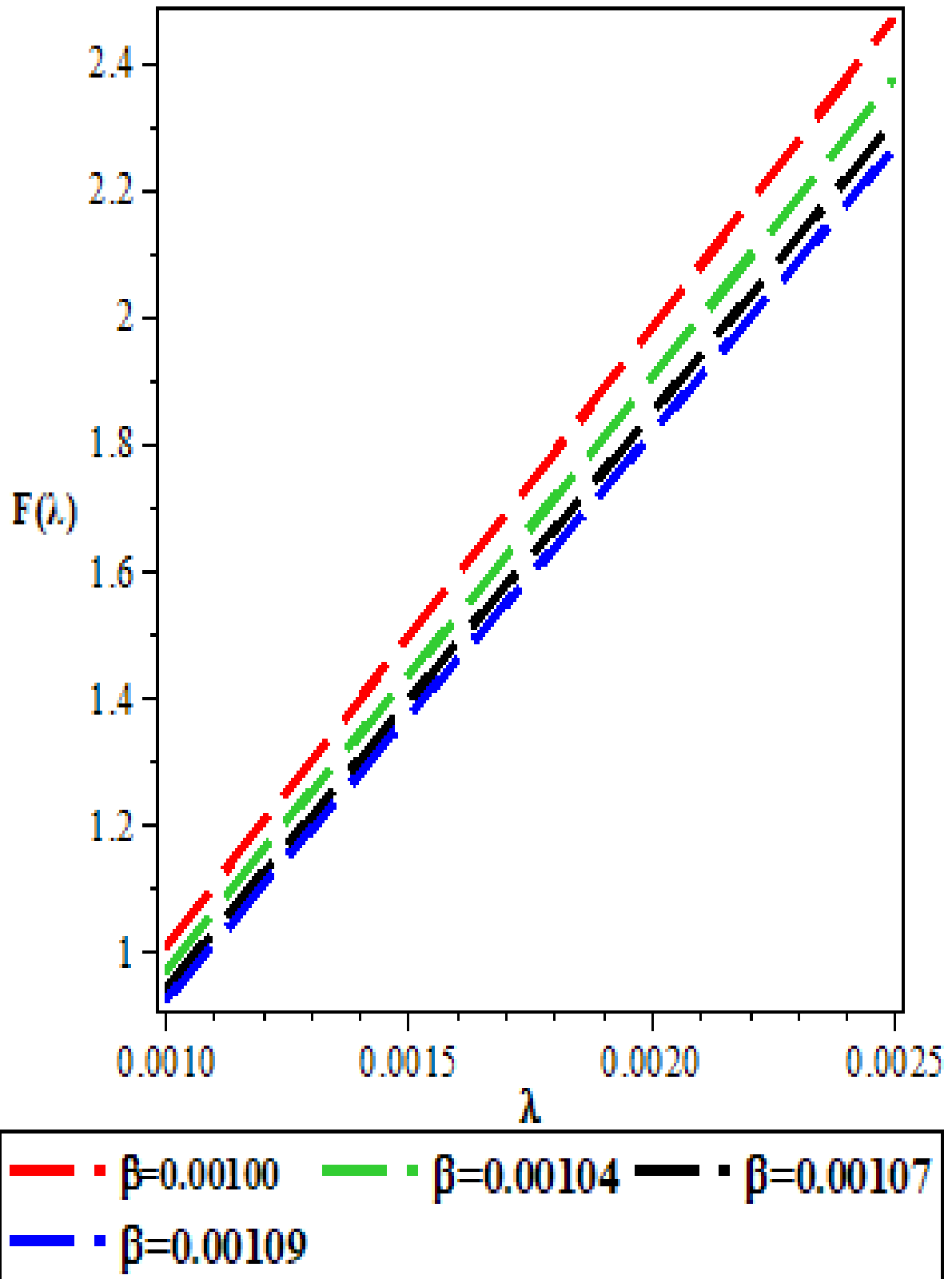


Figure 4.12: The plot of vibrational free energy (J) against maximum quantum state  $\lambda$  with varying  $\beta$  using equation (3.84)

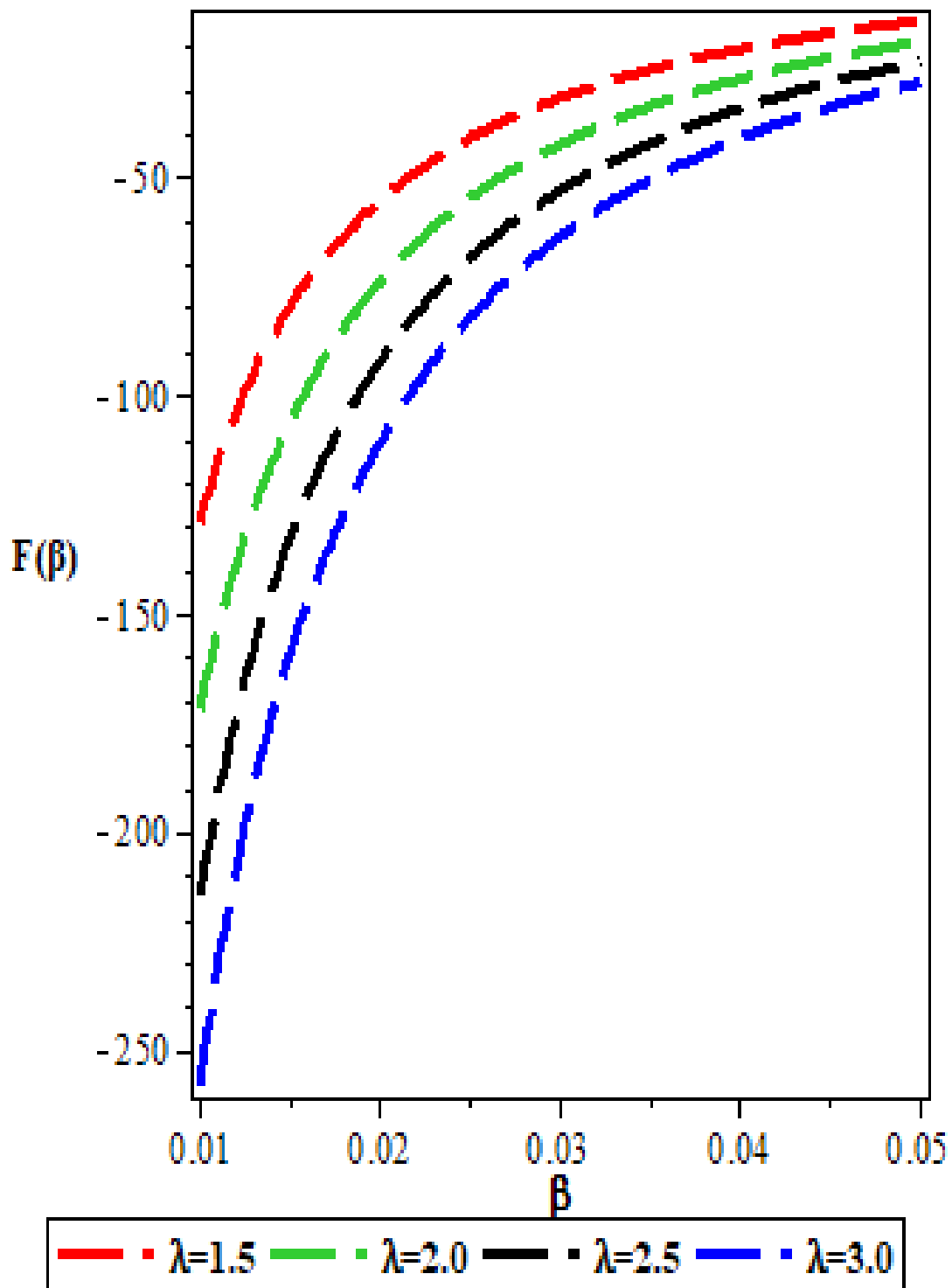


Figure 4.13: The plot of vibrational free energy ( $J$ ) against the temperature parameter  $\beta$  with varying  $\lambda$  using equation (3.84).

Table 4.1: Energy spectrum ( $E_{n,\ell}$ ) for different  $n$  and  $\ell$  states with four various values of the dissociation energy with  $\mu = h = 1, \alpha = 0.25 \text{ \AA}^{-1}, r_e = 0.20 \text{ \AA}, A = \frac{\lambda_o}{2}, B = 2(1 - \lambda_o), C = A+B+C$  and  $\lambda_o = 2$ .

$n$	$\ell$	$D_e = 5$	$D_e = 10$	$D_e = 15$	$D_e = 20$
0	0	3.977598	6.798288	9.109638	11.11615
1	0	4.809524	9.108668	13.05829	16.74890
	1	4.960983	9.609369	13.95089	18.03931
2	0	4.976040	9.723415	14.24875	18.59454
	1	4.999968	9.896182	14.59865	19.13354
	2	4.975467	9.985643	14.84931	19.57862
3	0	4.998604	9.936060	14.72396	19.38474
	1	4.973068	9.989806	14.87376	19.63950
	2	4.914077	9.996149	14.97331	19.85286
	3	4.829183	9.955367	14.99985	19.96640
4	0	4.963711	9.997845	14.92583	19.76044
	1	4.910165	9.993944	14.98133	19.88121
	2	4.826913	9.952550	14.99944	19.97229
	3	4.721396	9.876708	14.96871	19.99997
	4	4.596529	9.772933	14.89798	19.97316
5	0	4.895582	9.984638	14.99534	19.93525
	1	4.821832	9.946315	14.99782	19.98214
	2	4.718669	9.872484	14.96506	19.99961
	3	4.594756	9.769884	14.89453	19.97053
	4	4.452478	9.643210	14.79210	19.90024
	5	4.292898	9.495313	14.66266	19.79563
6	0	4.803143	9.925703	14.98878	19.99679
	1	4.712578	9.863310	14.95702	19.99765
	2	4.591609	9.764530	14.88850	19.96582
	3	4.450480	9.639598	14.78754	19.89565
	4	4.291478	9.492659	14.65910	19.79163
	5	4.115506	9.325890	14.50671	19.65851
	6	3.923026	9.140586	14.33274	19.49987
7	0	4.690304	9.834264	14.93217	19.98641
	1	4.584588	9.752979	14.87571	19.95556
	2	4.446934	9.633267	14.77961	19.88766
	3	4.289261	9.488538	14.65360	19.78546
	4	4.113949	9.322928	14.50261	19.65363
	5	3.921850	9.138317	14.32953	19.49591

	6	3.713375	8.935753	14.13619	19.31497
	7	3.488754	8.715886	13.92380	19.11270
8	0	4.559001	9.717008	14.83890	19.92568
	1	4.439029	9.619654	14.76300	19.87108
	2	4.285328	9.481320	14.64407	19.77484
	3	4.111518	9.318331	14.49627	19.64613
	4	3.920157	9.135061	14.32493	19.49026
	5	3.712105	8.933285	14.13264	19.31052
	6	3.487753	8.713926	13.92095	19.10908
	7	3.247313	8.477537	13.69085	18.88742
	8	2.990915	8.224476	13.44300	18.64662

Table 4.2: Energy spectrum ( $E_{n,\ell}$ ) for various states with four different values of the equilibrium bond

length  $r_e$  (Å) with  $\mu = h = 1$ ,  $D_e = 10$ ,  $A = \frac{\lambda_o}{2}$ ,  $B = 2(1 - \lambda_o)$ ,  $C = A+B+C$  and  $\lambda_o = 2$ .

State	$\alpha$	$r_e = 0.2$	$r_e = 0.4$	$r_e = 0.8$	$r_e = 1.0$
1s	0.05	8.822496	7.275723	5.246217	4.594310
	0.10	8.897665	7.388209	5.388441	4.743468
	0.15	8.970422	7.498611	5.529455	4.891884
	0.20	9.040758	7.606916	5.669226	5.039520
	0.25	9.108668	7.713107	5.807721	5.186332
	0.30	9.174145	7.817167	5.944906	5.332275
2s	0.05	9.441602	8.457590	6.777027	6.137691
	0.10	9.521127	8.594572	6.975023	6.352754
	0.15	9.594616	8.725541	7.167985	6.563434
	0.20	9.662051	8.850447	7.355807	6.769599
	0.25	9.723415	8.969242	7.538380	6.971111
	0.30	9.778689	9.081873	7.715589	7.167827
2p	0.05	9.643226	8.779637	7.064966	6.386061
	0.10	9.720650	8.919916	7.268475	6.606230
	0.15	9.788618	9.051703	7.465305	6.820566
	0.20	9.847129	9.174987	7.655407	7.029000
	0.25	9.896182	9.289757	7.838729	7.231458
	0.30	9.935776	9.395999	8.015214	7.427857
3s	0.05	9.696619	9.041944	7.712396	7.144368
	0.10	9.773022	9.187291	7.944278	7.403687
	0.15	9.838417	9.321038	8.165158	7.652694
	0.20	9.892774	9.443093	8.374818	7.891113
	0.25	9.936060	9.553358	8.573029	8.118653

	0.30	9.968245	9.651733	8.759556	8.335015
3p	0.05	9.796131	9.219469	7.897085	7.312206
	0.10	9.867573	9.364290	8.131821	7.574682
	0.15	9.923672	9.494396	8.353551	7.825115
	0.20	9.964420	9.609741	8.562130	8.063307
	0.25	9.989806	9.710281	8.757405	8.289049
	0.30	9.999824	9.795964	8.939212	8.502118
3d	0.05	9.873836	9.422222	8.187451	7.594783
	0.10	9.937062	9.564706	8.427501	7.863644
	0.15	9.978520	9.687037	8.650695	8.117081
	0.20	9.998215	9.789223	8.857010	8.355043
	0.25	9.996149	9.871273	9.046417	8.577464
	0.30	9.972324	9.933191	9.218880	8.784263
4s	0.05	9.824426	9.371662	8.324309	7.836124
	0.10	9.893731	9.516564	8.575011	8.123503
	0.15	9.945766	9.642809	8.806825	8.392553
	0.20	9.980486	9.750250	9.019384	8.642799
	0.25	9.997845	9.838734	9.212304	8.873750
	0.30	9.997797	9.908108	9.385192	9.084891
4p	0.05	9.879775	9.479154	8.449494	7.954597
	0.10	9.942095	9.621074	8.700983	8.243447
	0.15	9.981907	9.740609	8.931230	8.511953
	0.20	9.999196	9.837676	9.139956	8.759739
	0.25	9.993944	9.912183	9.326868	8.986409
	0.30	9.966133	9.964040	9.491660	9.191543
4d	0.05	9.925646	9.607029	8.649581	8.156289
	0.10	9.977483	9.743106	8.902396	8.448052
	0.15	9.999248	9.850394	9.129451	8.715544
	0.20	9.990937	9.928874	9.330616	8.958561
	0.25	9.952550	9.978519	9.505748	9.176880
	0.30	9.884082	9.999303	9.654687	9.370251
4f	0.05	9.956451	9.714053	8.868976	8.395042
	0.10	9.995277	9.841178	9.122506	8.690411
	0.15	9.994926	9.931178	9.343848	8.955828
	0.20	9.955401	9.984077	9.533043	9.191308
	0.25	9.876708	9.999901	9.690121	9.396847
	0.30	9.758852	9.978673	9.815103	9.572422

Table 4.3: Energy spectrum ( $E_{n,\ell}$ ) for different  $n$  and  $\ell$  states with four various values of the screening

parameter,  $\mu = h = 1$ ,  $r_e = 0.20 \text{ \AA}$ ,  $D_e = 10$ ,  $A = \frac{\lambda_o}{2}$ ,  $B = 2(1 - \lambda_o)$ ,  $C = A+B+C$  and  $\lambda_o = 2$ .

$n$	$\ell$	$\alpha = 0.05$	$\alpha = 2.5$	$\alpha = 5.0$	$\alpha = 7.0$
0	0	6.607311	8.567361	9.720312	9.999578
1	s0	8.822496	9.531990	3.192581	-8.15051
	1	9.324380	7.531311	-5.767980	-24.4169
2	0	9.441602	5.857724	-15.81960	-49.5725
	1	9.643226	2.268525	-29.33370	-73.4512
	2	9.785762	-3.847690	-53.11610	-117.376
3	0	9.696619	-0.17753	-42.9711	-107.067
	1	9.796131	-4.97132	-60.2859	-137.318
	2	9.873836	-12.5903	-89.4150	-190.881
	3	9.923901	-22.2238	-127.140	-262.314
4	0	9.824426	-8.07204	-77.1356	-178.482
	1	9.879775	-13.9508	-97.9959	-214.648
	2	9.925646	-22.9920	-132.262	-277.402
	3	9.956451	-34.1305	-175.687	-359.450
	4	9.976389	-47.0594	-226.692	-457.320
5	0	9.896196	-17.6642	-117.916	-262.990
	1	9.929253	-24.5810	-142.217	-304.871
	2	9.957539	-35.0090	-181.524	-376.607
	3	9.976783	-47.6320	-230.588	-469.122
	4	9.989012	-62.0803	-287.485	-578.153
	5	9.996123	-78.2236	-351.453	-701.775
6	0	9.939295	-28.8891	-165.145	-360.220
	1	9.959789	-36.8226	-192.835	-407.717
	2	9.977460	-48.6197	-237.135	-488.326
	3	9.989247	-62.7162	-291.806	-591.225
	4	9.996204	-78.6773	-354.573	-711.364
	5	9.999461	-96.3513	-424.543	-846.473
	6	9.999852	-115.673	-501.312	-995.448
7	0	9.966066	-41.7167	-218.739	-469.984
	1	9.978859	-50.6559	-249.792	-523.045
	2	9.989650	-63.8127	-299.059	-612.465
	3	9.996327	-79.3764	-359.318	-725.700
	4	9.999488	-96.8460	-427.942	-856.912
	5	9.999842	-116.048	-503.905	-1003.48
	6	9.997938	-136.909	-586.743	-1164.15
	7	9.994173	-159.392	-676.222	-1338.24
8	0	9.982739	-56.1313	-278.655	-592.180
	1	9.990478	-66.0701	-313.057	-650.774
	2	9.996537	-80.5811	-367.275	-748.968
	3	9.999529	-97.6082	-433.110	-872.510
	4	9.999828	-116.584	-507.583	-1014.77
	5	9.997905	-137.312	-589.533	-1172.79
	6	9.994135	-159.711	-678.436	-1345.14

	7	9.988800	-183.737	-774.028	-1531.05
	8	9.982105	-209.370	-876.161	-1730.09

Table 4.4: Comparison of RKR ( $cm^{-1}$ ) data with calculated energies of  $Cs_2$  molecule and  $Li_2$  molecule.  $\sigma$  is calculated by using equation 4.1.

n	Cs <sub>2</sub>			Li <sub>2</sub>		
	RKR (Mesa <i>et al.</i> , 1998)	Calculated values	$\sigma$	RKR (Linton <i>et al.</i> , 1999)	Calculated values	$\sigma$
0	19,477.5507	19,477.55890	-0.008200	31.8570	31.80133823	0.05566177
1	19,506.2939	19,506.29961	-0.005710	90.4530	90.39141775	0.06158225
2	19,534.8916	19,534.87673	0.014870	142.523	142.4158566	0.10714340
3	19,563.3470	19,563.29044	0.056560	188.240	188.1839027	0.05609730
4	19,591.6634	19,591.54092	0.012248	227.679	227.4610980	0.21790200
5	19,619.8441	19,619.62831	0.215790	260.837	260.5359641	0.30103590
6	19,647.8922	19,647.55284	0.339360	287.665	287.3994373	0.26556270
7	19,675.8110	19,675.31463	0.496370	308.098	307.9456174	0.15238260
8	19,703.6037	19,702.91391	0.689790	322.155	322.2954606	-0.14046040
9	19,731.2736	19,730.35084	0.922760	330.170	330.7598462	-0.58984620
10	19,758.8239	19,757.62551	1.198800	333.269	333.5574895	-0.02884895

## 4.2 Discussion of Results

Figure 4.1 shows the computed result for variation in the principal quantum number ( $n$ ) for the energy eigenvalues against potential strength  $A$ . Two things are noticed here, firstly, as the potential strength  $A$  is decreasing from  $-10$  to negative infinity, the energy remains constant. Secondly, as the potential strength  $A$  is increasing from  $0$  to infinity, the energy also remains constant. It shows that the negative values of strength  $A$  increases as the energy eigenvalues also increases steadily while for the positive values of strength  $A$ , the energy eigenvalues also increase, however, two turning points are seen in the figure which are  $-6.5$  and  $-4.5$ . Figure 4.2 illustrates the graph of energy eigenvalues against potential strength  $B$  varying the principal quantum number. It is observed that as the energy of the system decreases the potential strength  $B$  increases. The energy eigenvalues increase as the negative values of strength  $B$  increase, but the energy eigenvalues decrease for the positive values of strength  $B$ , there is a turning point at potential strength  $B = -11.5$ . Also, the energy of the system rises to have a turning point at potential strength  $B = -9.5$  which tends to negative infinity.

Figure 4.3 illustrates the graph of energy eigenvalues against potential strength  $C$ , the graph is similar to figure 4.1 where the energy eigenvalues increase as the negative values of the strength  $C$  increase, however, for the positive values of the parameters, the energy eigenvalues decrease. Figure 4.4 shows the plot of vibrational partition function against the maximum quantum state. Various values of quantum state  $\lambda$  were plotted to show the effects of temperature parameter  $\beta$  on the partition function, it is observed that the variation of the vibrational partition function with the temperature parameter  $\beta$  has its highest value at  $0.012$ . However, as the values of the vibrational partition diverge in a monotonic manner, they tend

to converge on the maximum quantum state  $\lambda$  at the value of 0.000100. These figures imply that only when system temperature rises will the partition function increase.

Figure 4.5 displays the plot of vibrational partition function against the temperature parameter  $\beta$ . It is observed that the vibrational partition function of the system is decreasing in a monotonic manner when the quantum state and the temperature parameter increase, this reveals that as the system temperature rises, it leads to increase in the partition function of the system which is in line with what was done by Akanbi *et al.*, (2021). Figure 4.6 shows the variation of the maximum quantum state  $\lambda$  versus vibrational mean energy  $U$ . It is noticed that the vibrational mean energy of the temperature parameter of different values have the same values of the maximum quantum state and it is observed that the curve of the temperature parameter increases gradually to give a curve which has its maximum value at vibrational mean energy of 10 and maximum quantum state at 0.005, it shows that as the vibrational mean energy  $U$  (J) is increasing, the maximum quantum state is also increasing.

Figure 4.7 demonstrates the plot of the variation of vibrational mean energy  $U$  against the temperature parameter  $\beta$  respectively. It is observed that at different values of maximum quantum states, the vibrational mean energy tends to converge as the temperature of the system is rising slowly. It is noticed that when the maximum quantum state is having the lowest value that is when it has the highest vibrational mean energy. It is denoted that the higher the maximum quantum state  $\lambda$ , the lower the vibrational mean energy. Also, when the system's temperature continues to rise, the vibrational mean energy seems to approach each other.

Figure 4.8, displays the behaviour of the maximum quantum state and the vibrational specific heat capacity  $C$  are shown. It shows that as the vibrational specific heat capacity rises the maximum quantum state  $\lambda$  increases for some values which have a moment of turning point at the value of maximum quantum state  $\lambda = 4225$  which results in a gradual decrease at  $\lambda > 4225$

which implies that there is a limit at which the vibrational specific heat capacity cannot go beyond and at this point, the specific heat capacity starts diminishing. Figure 4.9 shows that the interaction between the temperature parameter  $\beta$  and the vibrational specific heat capacity  $C$ . It is seen that, as the temperature parameter increases, the vibrational specific capacity for different maximum quantum state  $\lambda$  diverges as temperature parameter increases which agrees with Okorie *et al.*, (2020).

Figure 4.10 explains the behaviour between vibrational entropy  $S$  and the maximum quantum state  $\lambda$ . It is discovered from the graph that the maximum quantum state  $\lambda$  increases as the vibrational entropy  $S$  rise for the various values of temperature parameter that are studied and it portrays a linear graph which denotes that the vibrational entropy  $S$  is directly proportional to the maximum quantum state of the different temperature parameter that is studied. Figure 4.11 shows the behaviour of vibrational entropy  $S$  against the temperature parameter  $\beta$ , various values of vibrational entropy are varied with different temperature parameter. It is observed from the graph that the higher the maximum quantum state, the higher the vibrational entropy which implies that the turning point of vibrational entropy for different values of maximum quantum state  $\lambda$  varies from each other. Nevertheless, the different values of vibrational entropy converge as the temperature parameter  $\beta$  increases which agrees with Akanbi *et al.*, (2021).

Figure 4.12 illustrates the effect of variation between the vibrational free energy  $F$  and the maximum quantum state  $\lambda$ . There is a direct variation between the vibrational free energy and the maximum quantum state  $\lambda$ . Figure 4.13, shows the plot of vibrational free energy  $F$  against temperature parameter  $\beta$ , the vibrational free energy shows a monotonic increase as the temperature parameter increase. A slight turning point is observed as the temperature parameter is increasing and tends to converge at 0.05. It is noticed from the graph that the higher the vibrational free energy, the lower the maximum quantum state  $\lambda$ . It is deduced that vibrational

free energy has a turning point at higher values of temperature parameter  $\beta$  which is in line with Akanbi *et al.*, (2021).

Table 4.1 gives the presentation of the energy spectrum for various values of dissociation energy at 5, 10, 15 and 20 respectively with equilibrium bond length of 0.20 with different values of principal quantum number and angular momentum quantum number. The lower the energy of dissociation, the lower the energy of the system as seen from the table. It is also observed that there is a direct variation between the quantum number and the energy eigenvalue of the system. In other words, as the quantum numbers are increasing, the energy eigenvalue of the system are also increasing as stated by Onate *et al.*, (2021).

Table 4.2 illustrates the variation of different states with different screening parameter and various equilibrium bond length of 0.2, 0.4, 0.8 and 1.0 of the energy spectrum equation (3.27). It is observed that for 1s state, as the screening parameter is increasing for the four different equilibrium bond length, the energy eigenvalues are also increasing which shows that there is a direct variation between the screening parameter and the energy eigenvalues. From 1s to 3s state with equilibrium bond length of 0.2, as the screening parameter is increasing, the energy eigenvalues is also increasing, however, as it reaches 4p States and the screening parameter reaches 0.30, the energy eigenvalues starts decreasing from 0.30 at equilibrium bond length of 0.2 which implies that starting from 4p states, the energy eigenvalues starts fluctuating at equilibrium bond length of 0.2 and 0.4. It is noticed from the table that initially, as the dissociation energy is increasing, the energy eigenvalues are increasing. But when the principal quantum number reaches 2 and the angular momentum quantum number increases. The energy eigenvalues are decreasing at dissociation energy of 5, but at dissociation energy of 10, on

reaching the radial quantum number of 3, it first increases and later decrease which implies that the eigenvalues are not stable again. It shows that when the energy of the system is low, the equilibrium bond separation is high, it also explains that as the screening parameter is increasing, the energy of the system is also increasing, and in other words, there is a direct variation between the screening parameter and the energy of the system which confirms the study by Dong *et al.*, (2008).

Table 4.3 represents the variation of different screening parameters with the dissociation energy of 10 and equilibrium bond length of 0.20, it is observed that when the principal quantum number and the azimuthal quantum number are increasing and the screening parameter is at 0.05, the eigenvalues first increases and towards the later part it first increases but later to decrease. It shows that it is only when the principal and azimuthal quantum number is 0 that the eigenvalues are increasing as the screening parameters are increasing. But at others, the eigenvalues are decreasing as the screening parameter is increasing.

Table 4.4 displays the comparison between the RKR data ( $\text{cm}^{-1}$ ) from Mesa *et al.*, (1998) with the calculated energies of the cesium dimer molecule. The computed RKR vibration energy and the experimental results are reported for cesium dimer and lithium dimer using equations (3.58) to equation (3.64), and the experimental data taken from Nikiforov and Uvarov (1988) and Tezcan and Sever (2008). For cesium dimer,  $D_e = 2722.28\text{cm}^{-1}$ ,  $r_e = 5.3474208 \text{ \AA}$ , and  $\omega_e = 28.8918\text{cm}^{-1}$  for lithium dimer,  $D_e = 2722.28\text{cm}^{-1}$ ,  $r_e = 4.173 \text{ \AA}$ , and  $\omega_e = 65.130\text{cm}^{-1}$ .

For both cesium dimer and lithium dimer, a deviation  $\sigma$  was calculated. For cesium dimer, deviation  $\sigma$  increases from the lowest degree of vibration to the highest level of vibration. The deviations from the lower levels of the lithium dimer rise to the first three lower levels of vibration, then the pattern shifts without any set format. Also, it is observed that as the

vibrational levels are increasing, the calculated energies for cesium dimer molecule are also increasing i.e., there is a direct variation. The same thing is noticed for lithium dimer molecule, it is also noticed that the deviation for cesium dimer is increasing as the vibrational levels are increasing which shows a similar behaviour with nitrogen molecule as reported by Onate *et al.*, (2021). However, the deviation for lithium dimer molecule first increase and afterwards there is a change in the pattern of deviation. The average deviation for each molecule was computed using a method to establish the approximation of comparing estimated and experimental values in equation (4.1) below.

$$\sigma_{av} = \frac{100}{N} \sum_v \left| \frac{E_{RKR} - E_{v0}}{E_{RKR}} \right|, \quad (4.1)$$

where  $E_{RKR}$  are the experimental values,  $E_{v0}$  is the value calculated and the number of the RKR data points of the experiment. The calculation shows an average 0.4415 percent divergence from the cesium dimer and 0.0007 percent from the lithium dimer. It is seen from these average deviations that the result for lithium dimer molecule agrees better than the result for cesium dimer molecule.

### 4.3 Findings

The findings from this work are as follows:

- (1) The addition of potential parameters has effects on the system. Potential strength A and potential strength C has similar effects. This resulted in the energy approaching a steady state as the potential strength A and C declined from -10 as it increases by 0, energy comes even close to a steady state. But as potential strength B increases, the energy of

the system gets close to negative infinity. Where  $A = \frac{\lambda_o}{2}$ ,  $B = 2(1 - \lambda_o)$ ,  $C = A+B+C$  and  $\lambda_o$  is 2.

- (2) As the temperature of the system increases, the partition function of the system also increases.
- (3) The vibrational mean energy attains its stability as there was gradual increase in the temperature of the system.
- (4) There was a direct variation between vibrational specific heat capacity and temperature parameter, however there is a turning point when maximum quantum state is at the value 4225 after which the vibrational specific heat capacity starts decreasing.
- (5) Increase in temperature parameter of the system makes the vibrational entropy to attain its stability.
- (6) There is a direct variation between the vibrational free energy and the temperature parameter.
- (7) The variation of cesium dimer and lithium dimer was calculated and the deviation from the lowest vibration level and the lithium dimer was found to increase from the lowest vibration level and to increase the deviation from the least vibrational level to the first three different levels after which the deviation pattern was unsatisfactory.

## CHAPTER FIVE

### SUMMARY, CONCLUSION AND RECOMMENDATION

#### 5.1 Summary

Using a straight forward Nikiforov-Uvarov approach, the Schrödinger equation obtained an approximate solution for the improved molecular attractiveness potential.

The equation energy and the matching functions of radial wave were achieved and the impact of the possible strength A, B and C on the attractive molecular potential were also observed on the energy eigenvalues and it was observed that potential strength A and C yielded the same result while potential strength B yielded a different result. The thermal properties such as vibrational partition function, vibrational mean energy, vibrational specific heat capacity, vibrational entropy, and vibrational free energy were studied using the molecular attractive potential. The study showed that as the system's temperature goes up, the vibrational partition function likewise goes up, for the vibrational mean free energy, it reduced when the temperature parameter rises and increased when the maximum quantum number increased. The specific capacity was also varied with the temperature parameter and it showed a direct variation. The vibrational entropy attains its stability as the temperature parameter was increased.

The Rydberg-Klein-Rees (RKR) of cesium dimer and lithium dimer was compared with the experimental values with the usage of parameters molecular spectroscopy. The values of the RKR for cesium dimers are 0.4415%, and the RKR for lithium dimer is 0.0007%. This suggests that the average deviation from the cesium dimer molecule is small. The result also shows that the average deviation computed agreed with the observed values.

## 5.2 Conclusion

A theoretical determination of Rydberg-Klein-Rees (RKR) values of some molecules with a four-parameter exponential-type molecular potential was considered in this study. The numerical study was carried out using maple software. From the study, the following deductions were made:

An approximate analytical solutions of molecular attractive potential energy models using parametric Nikiforov- Uvarov method was obtained; the thermodynamic properties of the molecular attractive potential were obtained mathematically.

Numerical procedures were employed to generate the eigenvalues and its corresponding wave functions; the spectroscopic parameters were inputted into the energy equation to obtain the calculated Rydberg-Klein-Rees values which were compared with the experimental values. The experimental results qualitatively agreed with the theoretical results

## 5.3 Recommendation

Further extension of the study is recommended by considering the spectroscopic parameters of other molecules to generate the values of Rydberg-Klein-Rees whether it will agree with the experimental results. Also, other solution techniques of Schrödinger equation can be employed to obtain the energy equation which will be used to generate eigenvalues.

## 5.4 Contributions to Knowledge

Horchani *et al.*, (2020) reported that till now, there has not been a principal method of using a potential energy function for modelling diatomic molecules, thereby making it difficult to find an appropriate potential that suits experimental data. However, this study has been able to contribute to the study of molecular physics by increasing the number of potentials numerically that can be used to verify experimental results.



## REFERENCES

- Agboola, D. (2010). Solutions to the Modified Pöschl–Teller Potential in D-Dimensions. *Chinese Physics Letters*, 27(4), 040301.
- Akanbi, T. A., Onate, C. A., and Oludoun, O. Y. (2021). Eigensolutions and thermodynamic properties of deformed and modified Morse potential model. *AIP Advances*, 11(4), 045213.
- Asim Gangopadhyaya, Jeffry Mallow, Constantin Rasinariu. (2018). Supersymmetric Quantum Mechanics. An Introduction. Second Edition. Published by World Scientific Publishing Singapore 1-104.
- Bera, P.K. (2013). Three-body interactions and the Landau levels using Nikiforov-Uvarov method. *PRAMANA Journal of Physics*, 81(2), 359-363.
- Dong, S. H. and Gu, X. Y. (2008). Arbitrary l state solutions of the Schrödinger equation with the Deng–Fan molecular potential. *Journal of Physics: Conference Series*. 96, 012109.
- Dong, S-H., Morales, D. and Garc'ia-Ravelo (2007). Exact Quantization rule and its application to physical potentials. *International Journal of Modern Physics*, 6(1), 189–198.
- Ebomwonyi, O., Onate, C.A., Ekong, S.A., and Onyeaju, M.C. (2019). Thermodynamic Properties for the Carbon Monoxide Molecule under the Influence of the Coulomb-Hulthen-Pöschl-Teller Potential. *Journal of Science and Technology Research* 1(1). 122-136.
- Eyube, E.S., Yabwa, D. and Wadata, U. (2020). Rotational- Vibrational eigen solutions of the D-dimensional Schrodinger equation for the improved Wei Potential. *FUDMA Journal of Sciences (FJS)*, 4(2), 269-288.

- Falaye, B. J., Oyewumi, K. J., Ikhdair, S. M., and Hamzavi, M. (2014). Eigensolution techniques, their applications and Fisher's information entropy of the Tietz–Wei diatomic molecular model. *Physica Scripta*, 89(11), 115204.
- Farout, M., Bassalat, A. and Ikhdair, S. (2020). Feinberg-Horodecki Exact Momentum States of Improved Deformed Exponential-Type Potential. *Journal of Applied Mathematics and Physics*, 8(8), 1496-1506.
- Feizi, H., Rajabi, A. A., and Shojaei, M. R. (2011). *Acta Physica Polonica B*, 42(10), 2143-2154.
- Hamzavi, M., Hassanabadi, H., and Rajabi, A. (2010). Exact solutions of Dirac equation with Hartmann potential by Nikiforov–Uvarov method. *International Journal of Modern Physics E*, 19(11), 2189–2197.
- Hamzavi, M., Rajabi, A. A., and Hassanabadi, H. (2012). The rotation–vibration spectrum of diatomic molecules with the Tietz–Hua rotating oscillator and approximation scheme to the centrifugal term. *Molecular Physics*, 110(7), 389–393.
- Horchani, R, Al- Kindi, N and Jelassi H., (2020). Ro-vibrational energies of caesium molecules with the Tietz- Hua oscillator. *Molecular Physics*. 119(4), 27-36.
- Hu, X.-T., Liu, J.-Y., and Jia, C.-S. (2013). The  $3^3 \Sigma_g^+$  state of  $CS_2$  molecule. *Computational and Theoretical Chemistry*, 1019, 137–140.
- Ikhdair, S. M., and Sever, R. (2008). Exact quantization rule to the Kratzer-type potentials: an application to the diatomic molecules. *Journal of Mathematical Chemistry*, 45(4), 1137–1152.
- Ikhdair, S. M. (2009). An improved approximation scheme for the centrifugal term and the Hulthén potential. *The European Physical Journal A*, 39(3), 307–314.

Ikhdaïr, S. M. (2012). Approximate 1-States of the Manning-Rosen Potential by Using Nikiforov-Uvarov Method. *International Scholarly Research Network ISRN Mathematical Physics*, 1(1), 1–20.

Ikot, A., Maghsoodi, E., Ibanga, E., Ituen, E., & Hassanabadi, H. (2016). Bound States of the Dirac Equation for Modified Mobius Square Potential Within the Yukawa-Like Tensor Interaction. *Proceedings of the National Academy of Sciences, India Section A: Physical Sciences*, 86(3), 433–440.

Ikot, A.N., Chukwuocha, E.O., Onyeaju, M.C., Onate, C. A., Ita, B.I and Udoh, M.E. (2018). Thermodynamics properties of diatomic molecules with general molecular potential. *Pramana-Journal of Physics*, 90(22), 22-30.

Ikot, A. N., Okorie ,U. S, Ramadan, S. and Rampho, G. J. (2019). Eigensolution, expectation values and thermodynamic properties of the screened Kratzer potential. *The European Physical Journal Plus*, 134(8), 34-42.

Ismail ,M.E.H and Saad, N. (2020). The Asymptotic Iteration Method Revisited. *Journal of Mathematical Physics*, 61(33), 5-12.

Ita, B. I. and Ikeuba, A. I. (2013). Solutions to the Schrödinger Equation with Inversely Quadratic Yukawa Plus Inversely Quadratic Hellmann Potential Using Nikiforov-Uvarov Method. *Journal of Atomic and Molecular Physics*. 2(3), 1–4.

Ita, B.I and Hitler, L. (2017). Bound State Solutions of the s-wave Schrodinger Equation for Generalized Woods-Saxon plus Mie-Type Nuclei Potential within the framework of Nikifarov-Uvarov Method. *World Scientific News*, 77(2), 378-384.

Jaeger, G. (2014). What in the (quantum) world is macroscopic? *American Journal of Physics*. 2(9), 896–905.

Jia, C.-S, Liu, J.-Y and Wang, P.-Q. (2008). A new approximation scheme for the centrifugal term and the Hulthén potential *Physics Letters A*. 372(3), 4779-4782.

Jia, C.-S., Diao, Y.-F., Liu, X.-J., Wang, P.-Q., Liu, J.-Y., and Zhang, G.-D. (2012). Equivalence of the Wei potential model and Tietz potential model for diatomic molecules. *The Journal of Chemical Physics*, 137(1), 014101.

Jia, C.-S., Zhang, L.-H., and Peng, X.-L. (2017). Improved Pöschl-Teller potential energy model for diatomic molecules. *International Journal of Quantum Chemistry*, 117(14), e25383.

Liu, J.-Y., Hu ,X.-T. and Jia ,C.-S. (2014). Molecular energies of the improved Rosen–Morse potential energy model. *Canadian Journal of Chemistry*. 92(1), 40–44.

Lucha, W. and Schöberl, F. F. (1999). Solving the Schrödinger equation for bound states with Mathematica 3.0. *International Journal of Modern Physics C* 10(4), 607–620

Mesa, A.D.C., Quesne, C., Smirnov, Y.F. (1998). Generalized Morse potential: symmetry and satellite potentials, *Journal of Physics*. 31(3), 321-335.

Nikiforov, A.F. and Uvarov, V.B. (1988) *Special Functions of Mathematical Physics*. Birkhäuser, Basel.205-295.

Nugraha, D. A., Suparmi, A., Cari, C., and Pratiwi, B. N. (2017). Asymptotic iteration method for analytical solution of Klein-Gordon equation for trigonometric Pöschl-Teller potential in D-dimensions. *Journal of Physics: Conference Series*, 795(1), 20-25.

Okon, I.B and Popoola, O. (2015). Bound-state solution of Schrödinger equation with Hulthén plus generalized exponential coulomb potential using Nikiforov-Uvarov method. *International Journal of Recent Advances in Physics (IJRAP)*. 4(3), 1-12.

- Okorie, U. S., Ikot, A. N., Edet, C. O., Akpan, I. O., Sever, R., and Rampho, R. (2019). Solutions of the Klein Gordon equation with generalized hyperbolic potential in D-dimensions. *Journal of Physics Communications*, 23(5), 23-29.
- Okorie, U. S., Ibekwe, E. E., Ikot, A. N., Onyeaju, M. C., and Chukwuocha, E. O. (2018). Thermodynamic Properties of the Modified Yukawa Potential. *Journal of the Korean Physical Society*. 73(9), 1211–1218.
- Okorie, U. S., Ikot, A. N., Chukwuocha, E. O., and Rampho, G. J. (2020). Thermodynamic properties of improved deformed exponential-type potential (IDEP) for some diatomic molecules. *Results in Physics*, 17, 103078.
- Omugbe, E., Osafire, O. E., Okon, I. B., and Onyeaju, M. C. (2020). Energy Spectrum and the properties of the Schiöberg potential using the WKB approximation approach. *Molecular Physics*, 119 (4), 1–12.
- Onate, C. A. and Idiodi, J. O. A. (2016). Fisher Information and Complexity Measure of Generalized Morse Potential Model. *Communications in Theoretical Physics*, 66(3), 275–279.
- Onate, C.A and Onyeaju, M.O (2017). Dirac particles in the field of Frost Musulin diatomic potential and the thermodynamic properties via parametric Nikiforov- Uvarov method. *Sri Lankan Journal of Physics*. 17(7),1-17.
- Onate, C.A, Onyeaju, M.A, Ikot, A.N, John, O.E and Idiodi, O.A., (2019). Fisher Information and uncertainty relations for potential family. *International Journal of Quantum Chemistry*. 119 (19), 10-19.
- Onate, C. A., Onyeaju, M. C., Okorie, U. S. and Ikot, A. N. (2020). Thermodynamic functions for Boron nitride with q-deformed exponential-type potential. *Results in Physics*. Results in Physics 16(10), 29-39.

Onate, C. A., and Akanbi, T. A. (2021). Solutions of the Schrödinger equation with improved Rosen Morse potential for nitrogen molecule and sodium dimer. *Results in Physics*, 22, 103961.

Oyewumi, K. J., Falaye, B. J., Onate, C. A., Oluwadare, O. J., and Yahya, W. A. (2013). Thermodynamic properties and the approximate solutions of the Schrödinger equation with the shifted Deng–Fan potential model. *Molecular Physics*, 112(1): 127–141.

Pahlavani, Mohammad Reza (2012). *Theoretical Concepts of Quantum Mechanics*. Published by InTech, Janeza Trdine 9, 51000 Rijeka, Croatia.

Richard ,F., Robert, L. and Matthew, S. (1964). *The Feynman Lectures on Physics* . California Institute of Technology. ISBN 978-0201500646. Archived from the original on 2018-11-26. Retrieved 2017-01-03. 3(1.1).

Schrödinger, E. (1926). An undulatory theory of the mechanics of atoms and molecules. *Physical Review*. 28 (6):1049-S1070. Archived from the original (PDF) on 17 December 2008.

Tang, H.-M., Liang, G.-C., Zhang, L.-H., Zhao, F., and Jia, C.-S. (2014). Diatomic molecule energies of the modified Rosen–Morse potential energy model. *Canadian Journal of Chemistry*, 92(4), 341–345.

Tezcan, C. and Sever, R. (2008). A General Approach for the Exact Solution of the Schrödinger Equation. *International Journal of Theoretical Physics*. 48(2), 337–350.

Udoh, M. E., Okorie, U. S., Ngwueke, M. I., Ituen, E. E. and Ikot, A. N. (2019). Rotation-vibrational energies for some diatomic molecules with improved Rosen–Morse potential in D-dimensions. *Journal of Molecular Modelling*. 25(6), 1-7.

Wei, G.-F., & Dong, S.-H. (2010). Pseudospin symmetry in the relativistic Manning–Rosen potential including a Pekeris-type approximation to the pseudo-centrifugal term. *Physics Letters B*, 686(4-5), 288–292.

Williams, B.W. and Poullos, D.P. (1993). A simple method for generating exactly solvable quantum mechanical potentials. *European Journal of Physics*. 11(1), 222-226

Yahya, W. A. and Oyewumi, K. J. (2016). Thermodynamic properties and approximate solutions of the  $\ell$ -state Pöschl–Teller-type potential. *Journal of the Association of Arab Universities for Basic and Applied Sciences*. 21(1), 53–58.

Zettili, N. (2009). Quantum mechanics: concepts and applications. Second edition. John Wiley and Sons, Ltd. United Kingdom.10-102

Zhang, L.-H, Li ,X.-P and Jia, C.-S., (2010). Approximate solutions of the Schrödinger equation with the Generalized Morse Potential Model including the centrifugal term. *International Journal of Quantum Chemistry*. 111 (2011),1870-1878.